# *Hp* Clouds–A Meshless Method to Solve Boundary-Value Problems

C. Armando Duarte *
J. T. Oden †

TICAM - Texas Institute for Computational and Applied Mathematics
The University of Texas at Austin
Taylor Hall 2.400
Austin, Texas, 78712, U.S.A.

**TICAM Report 95-05**
**(Revised)**

**Abstract**

A new method to build discrete models of boundary value problems is presented. The *hp* cloud method is applicable to arbitrary domains and employs only a scattered set of nodes to build approximate solutions to BVPs. This new method uses radial basis functions of varying size of supports and with polynomial reproducing properties of arbitrary order. The approximating properties of the *hp* cloud functions are investigated in this paper and a number of theorems concerning these properties are presented. Moving least-squares interpolants are used to build a partition of unity on the domain of interest. These functions are then used to construct, at a very low cost, trial and test functions for Galerkin approximations. The method exhibits very high rate of convergence and has a greater flexibility than traditional *hp* finite element methods. Several numerical experiments in 1-D and 2-D are also presented.

*Research Assitant, TICAM. e-mail: armando@ticam.utexas.edu
†Professor, Director, TICAM. e-mail: oden@ticam.utexas.edu

# 1 Introduction

In most large-scale numerical simulations of physical phenomena, a large percentage of the overall computational effort is expended on technical details connected with meshing. These details include, in particular, grid generation, mesh adaptation to domain geometry, element or cell connectivity, grid motion and separation to model fracture, fragmentation, free surfaces, etc. Moreover, in most computer-aided design work, the generation of an appropriate mesh constitutes, by far, the costliest portion of the computer-aided analysis of products and processes.

These are among the reasons that interest in so-called meshless methods has grown rapidly in recent years. Most meshless methods require a scattered set of nodal points in the domain of interest. In these methods there may be no fixed connectivities between the nodes, unlike the finite element or finite difference methods. This feature has significant implications in modeling some physical phenomena that are characterized by a continuous change in the geometry of the domain under analysis. The analysis of problems such as crack propagation, penetration and large deformations, can, in principle, be greatly simplified by the use of meshless methods. A growing crack, for example, can be modeled by simply extending the free surfaces which correspond to the crack [5]. The analysis of large deformation problems by, e.g., finite element methods, may require the continuous remeshing of the domain to avoid the break down of the calculation due to excessive mesh distortion. The use of a method that does not require successive remeshings, even after very large deformations have occurred, can dramatically simplify the modeling of this class of problems. Even in problems where only one mesh is needed for an analysis, mesh generation can be a far more time consuming and expensive task than the construction and solution of the discrete set of equations. Therefore, a method that can deliver accurate solutions to boundary-value problems without the need of explicitly partitioning the domain could have a positive impact on many aspects of computer simulations.

Among the first methods of these types used in numerical solution of boundary-value problems are the Generalized Finite Difference Methods (GFDM) of Liszka and Orkisz [27–29] and Smoothed Particle Hydrodynamics (SPH) [17, 34, 37, 38]. More recently, the importance of meshless methods is reflected by the number of new methods that have been proposed: The Diffuse Element Method (DEM) [40], The Element Free Galerkin Method (EFGM) [5,6], Wavelet Galerkin Methods (WGM) [3, 18, 43], Multiquadrics [21, 22], Reproducing Kernel Particle Methods (RKPM) [30, 31] and The Free Mesh Method

(FMM) [50].

Behind all these methods there is an underlying approximation technique that can handle arbitrarily spaced data on complex domains; the DEM and the EFGM are based on the Moving Least Square Method (MLSM) [25,26]; the kernel estimates of Monaghan [37] funds the basis for the SPH method. Therefore the first step in understanding any of these methods is the study of the underlying approximation (interpolation) technique and properties. Also, the study of the corresponding approximation technique of a meshless method can reveal its strength and weakness and reveal methods for improvement.

The problem of interpolation to arbitrarily spaced data is encountered in such areas as geodesy, geophysics, mapping, geography, hydrology, etc [19]. Therefore the development of a new approximation technique that can handle arbitrarily scattered data can contribute not only to the development of a new meshless method to solve boundary-value problems, but can also benefit many other areas.

Duarte [14] has prepared a comprehensive review of the meshless methods found in the literature. The connection among the methods and the corresponding underlying approximation technique were also investigated. The conclusion of that study is that, from the point of view of accuracy and efficiency, in spite of the variety of the meshless methods found in the literature, all the reviewed methods have serious limitations that, in most situations, can negate some of the advantages of these methods over more reliable methods such as *hp* finite element methods.

The SPH method appears to be one of the most flexible of the meshless methods and is simple to implement. The SPH method uses collocation at the nodes to build a discrete set of equations governing the problem [45] and, therefore, does not require a background quadrature scheme. The price of this simplicity and flexibility is the poor accuracy of the method. A large number of nodes are usually required to achieve reasonably accuracy in practical applications. The reason for this poor accuracy is that the kernel estimation technique used in the SPH method is equivalent to the use of Shephard interpolants [14, 33] which are well known for its poor accuracy [16]. Another problem of the SPH method is the spatial instability of the method, often known as tensile instability [45].

The EFGM [5, 6] and the DEM [40] have only two major differences [5, 14]: the EFGM includes certain terms in the derivatives of the interpolants which are omitted in the DEM and the EFGM employs Lagrange multipliers to enforce essential boundary conditions. Both methods use moving least square functions [25] as a means of spatial discretization. These functions are used to construct a finite dimensional subspace of, e.g., $H^1(\Omega)$ and then a Galerkin method is employed to find an approximate solution in this subspace [5, 6]. Both methods have some very attractive characteristics. The MLSM can produce functions with any degree of regularity, even $C^\infty(\Omega)$, at no extra cost. Therefore the EFGM can give, e.g., $C^1(\Omega)$ approximations of the solution of a second order BVP. Thus the smoothing of fluxes used in the FEM to obtain a continuous flux is completely unnecessary in the EFGM and DEM. These methods are applicable to arbitrary domains and Belytschko and colleagues [5,6,32] have reported that the EFGM is very accurate and can achieve higher rates of convergence than the finite element method. The method does not exhibit volumetric locking and performance apparently is only minimally affected by irregular placement of nodes. The main drawbacks of the method is the cost of building the moving least square functions and the need of a background quadrature scheme to evaluate the integrals that appears in the weak forms used by the Galerkin method. Another difficulty appears in the construction of the MLS functions. There must be an increase in the size of the support of these functions if one wants to increase the polynomial degree that the MLS functions can reproduce. Also there are some nodal arrangements that can break down the algorithm used to construct the MLS functions [14].

Duarte [14] has shown that the underlying interpolation technique used in the generalized finite difference method [27–29] has many similarities with the MLS method and are equivalent under special circumstances. The GFDM is more flexible than the EFGM since, like in the SPH method, a collocation process at the nodes is used to construct the discrete set of equations governing the problem and therefore no other quadrature scheme is needed. Nonetheless, the method also has the limitations imposed by the use of a MLS like approximation technique. Another drawback of the method is the low degree of regularity of the underlying basis functions which may not even be continuous. The literature on wavelet based methods suggests that these methods are generally limited to particular domain geometries, such as rectangular domains, and their application to more general domains requires the use of special techniques, such as the fictitious domain method [43].

Another limitation of the meshless methods found in the literature is that none of them, except the wavelet method in one dimension [18] and the GFDM, has a rich mathematical background to justify their use. That is, mathematical proofs of conditions sufficient to guarantee that these methods will converge to the true solution are not available.

This paper presents a new family of meshless methods for the solution of boundary-value problems. The *hp* cloud method is applicable to arbitrary domains and employs only a scattered set of nodes to build approximate solutions to boundary-value problems. The method uses radial basis functions of varying size of supports and with polynomial reproducing properties of arbitrary order. The first numerical experiments with this technique show very promising results.

The next sections of this paper describe in detail the *hp* cloud method. Following this Introduction, Section 2 introduces the *hp* cloud family of spaces $\mathcal{F}_N^{k,p}$ . *a-priori* error estimates for the *h* version of the method are presented in Section 3. Finally, Sections 4 and 5 present the results of numerical experiments involving approximation of functions by *hp* clouds and solution of boundary-value problems in one and two dimensions.

# 2 *Hp* Clouds: High Order Approximation of Scattered Data

## 2.1 Introduction

In this section a technique for approximating functions defined on an open bounded domain $\Omega \in \mathbb{R}^n, n = 1, 2$ or 3 is presented. The method employs only an arbitrarily scattered set of nodes belonging to $\Omega$. The major motivation for the development of the method is to construct accurate solutions to boundary value problems without the need of explicitly partitioning the domain of interest in many smaller suitable subdomains, as is done in the finite element, finite difference and finite volume methods. Nonetheless, the *hp* cloud technique has a much broader range of application.

## 2.2 Signed Partition of Unity

We begin by introducing some notation used throughout this paper:

We assume that $\Omega$ is an open smooth domain in $\mathbb{R}^n$, $n = 1, 2$ or 3. $\boldsymbol{Q}_N$ will denote an *arbitrarily* chosen set of $N$ nodes $\boldsymbol{x}_\alpha \in \Omega$

$$\boldsymbol{Q}_N = \{\boldsymbol{x}_1, \boldsymbol{x}_2, \ldots, \boldsymbol{x}_N\},\ \boldsymbol{x}_\alpha \in \Omega$$

The set $\boldsymbol{Q}_N$ is then used to define a finite open covering $\mathcal{T}_N := \{\omega_\alpha\}_{\alpha=1}^N$ of $\Omega$ composed of $N$ balls $\omega_\alpha$ centered at the points $\boldsymbol{x}_\alpha$, $\alpha = 1, \ldots, N$, where

$$\omega_\alpha := \{\boldsymbol{y} \in \mathbb{R}^n : \|\boldsymbol{x}_\alpha - \boldsymbol{y}\|_{\mathbb{R}^n} < h_\alpha\}$$

$$\bar{\Omega} \subset \bigcup_{\alpha=1}^{N} \omega_\alpha$$

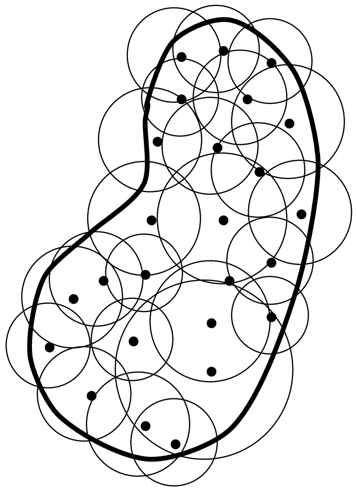

Figure 2.1: Open covering with balls centered at the nodes.

One fundamental step in the approximation of functions by the *hp* cloud method is the construction of a *signed partition of unity* . A class of functions $\{\varphi_\alpha\}_{\alpha=1}^{N}$ is called a signed partition of unity with respect to the open covering $\mathcal{T}_N$ if it possesses the following properties:

**1)** $\varphi_\alpha \in C_0^\infty(\omega_\alpha), \qquad 1 \leq \alpha \leq N$

**2)** $\sum_{\alpha=1}^{N} \varphi_\alpha(\boldsymbol{x}) = 1, \qquad \forall\, \boldsymbol{x} \in \Omega$

A signed partition of unity is referred to as a $\boldsymbol{P}$ - *reducible system for the set* $\boldsymbol{Q}_N$ if given any set $\boldsymbol{P}$ of $m$ linearly-independent functions $\boldsymbol{P} = \{P_1, P_2, ..., P_m\}$, $P_j : \mathbb{R}^n \to \mathbb{R}$, a signed partition of unity can be constructed such that

$$P_j(\boldsymbol{x}) = \sum_{\alpha=1}^{N} P_j(\boldsymbol{x}_\alpha)\varphi_\alpha(\boldsymbol{x}) \ , \ \boldsymbol{x} \in \Omega$$

### 2.2.1 Construction of a Signed Partition of Unity

There is no unique way to build a signed partition of unity as defined above. In the *hp* cloud method we use the following approach:

Let $\mathcal{W}_\alpha : I\!R^n \to I\!R$ denote a **weight function** that belongs to the space $C_0^\infty(\omega_\alpha)$ with the following properties:

- $\mathcal{W}_\alpha(\boldsymbol{y}) \geq 0 \qquad \forall\ \boldsymbol{y}\ \in \Omega$
- $\mathcal{W}_\alpha(\boldsymbol{y}) := W_\alpha(\boldsymbol{y} - \boldsymbol{x}_\alpha)$

where the functions $W_\alpha \in C_0^\infty(B_{h_\alpha})$ and are defined over a ball $B_{h_\alpha}$ of radius $h_\alpha$ centered at the origin

$$B_{h_\alpha} = \{\boldsymbol{x} \in I\!R^n : \|\boldsymbol{x}\|_{I\!R^n} < h_\alpha\}$$

Next we introduce a family of functionals defined over continuous functions defined on $\Omega$ by

$$(f, g)_{\mathbf{y}} := \sum_{\alpha=1}^{N} \mathcal{W}_\alpha(\boldsymbol{y}) f(\boldsymbol{x}_\alpha) g(\boldsymbol{x}_\alpha), \qquad f, g : \Omega \to I\!R,\ \ f, g \in C^0(\Omega) \tag{2.1}$$

Given a set of $m$ functions $\boldsymbol{P} = \{P_1, P_2, ..., P_m\}$, $P_i : \Omega \to I\!R$, $P_i \in C^0(\Omega)$ for $i = 1, \ldots, m$, we assume that the set of nodes $\boldsymbol{Q}_N$, the open covering $\mathcal{T}_N$ and the weight functions $\mathcal{W}_\alpha$ are such that the matrix $(P_k, P_l)_{\mathbf{x}}$ is positive definite for all points $\boldsymbol{x} \in \Omega$. This hypothesis is formalized next.

**Assumption 2.1** *Given a set of $m$ functions $\boldsymbol{P} = \{P_1, P_2, ..., P_m\}$, $P_i : \Omega \to I\!R$, $P_i \in C^0(\Omega)$ for $i = 1, \ldots, m$, the weight functions $\mathcal{W}_\alpha$ defined above and the functions $P_i$ are such that $\forall\ \boldsymbol{x} \in \bar{\Omega}$ there holds*

$$\sum_{k=1}^{m} a_k (P_k, P_l)_{\mathbf{x}} \equiv 0 \ \ \text{for } l = 1, \ldots, m \quad \Longleftrightarrow \quad a_k \equiv 0 \ \ \text{for } k = 1, \ldots, m.$$

∎

The following result is due to Ainsworth [2]

**Proposition 2.2** *If the Assumption 2.1 holds then the functional $(.,.)_{\mathbf{x}}$ defined in (2.1) is an inner product on span($\boldsymbol{P}$).*

**Proof:**

Let $f \in span(\boldsymbol{P})$. Then

$$(f, f)_{\mathbf{x}} = \sum_{\alpha=1}^{N} \mathcal{W}_\alpha(\boldsymbol{x}) f(\boldsymbol{x}_\alpha)^2 \geq 0$$

with equality iff

$$\mathcal{W}_\alpha(\boldsymbol{x})f(\boldsymbol{x}_\alpha) = 0 \qquad for\ \alpha = 1,\ldots,N$$

thus

$$\mathcal{W}_\alpha(\boldsymbol{x})f(\boldsymbol{x}_\alpha)P_k(\boldsymbol{x}_\alpha) = 0 \qquad for\ \alpha = 1,\ldots,N,\ \ k = 1,\ldots,m$$

Since $f \in span(\boldsymbol{P})$, write

$$f(\boldsymbol{x}) = \sum_{l=1}^{m} a_l P_l(\boldsymbol{x}) \qquad \rightarrow \qquad f(\boldsymbol{x}_\alpha) = \sum_{l=1}^{m} a_l P_l(\boldsymbol{x}_\alpha)$$

then

$$\begin{aligned}
\mathcal{W}_\alpha(\boldsymbol{x})\sum_{l=1}^{m} a_l P_l(\boldsymbol{x}_\alpha)P_k(\boldsymbol{x}_\alpha) &= 0 \qquad for\ \alpha = 1,\ldots,N,\ \ k = 1,\ldots,m \\
\sum_{\alpha=1}^{N}\mathcal{W}_\alpha(\boldsymbol{x})\sum_{l=1}^{m} a_l P_l(\boldsymbol{x}_\alpha)P_k(\boldsymbol{x}_\alpha) &= 0 \qquad for\ k = 1,\ldots,m \\
\sum_{l=1}^{m} a_l \sum_{\alpha=1}^{N}\mathcal{W}_\alpha(\boldsymbol{x})P_l(\boldsymbol{x}_\alpha)P_k(\boldsymbol{x}_\alpha) &= 0 \qquad for\ k = 1,\ldots,m \\
\sum_{l=1}^{m} a_l (P_l, P_k)_{\mathbf{x}} &= 0 \qquad for\ k = 1,\ldots,m
\end{aligned}$$

By assumption this implies that $a_l \equiv 0$ and hence $f \equiv 0$. The remaining conditions are easily checked ∎

The next theorem gives us necessary, and in some cases sufficient, conditions for the satisfaction of Assumption 2.1.

**Theorem 2.3** *A necessary condition for the satisfaction of the Assumption 2.1 is that for any $\boldsymbol{y}, \in \bar{\Omega}$ there exist indices $\alpha_1, \ldots, \alpha_k$, $k \geq \#\boldsymbol{P} = m$, dependent on $\boldsymbol{y}$, such that*

$$\boldsymbol{y} \in \bigcap_{j=1}^{k} supp(\mathcal{W}_{\alpha_j}) \tag{2.2}$$

*If $\#\boldsymbol{P} = 1$, then the above condition is also sufficient. If $\bar{\Omega} \subset \mathbb{R}^2$ and $\boldsymbol{P} = \{1, x, y\}$ and in addition to the above condition $\boldsymbol{x}_{\alpha_1}, \ldots, \boldsymbol{x}_{\alpha_k}$ contains a subset of 3 points not aligned, then the above condition is also sufficient.*

**Proof:**

Let $\boldsymbol{y}$ be an arbitrary point in $\bar{\Omega}$ and the indices $\alpha_1, \ldots, \alpha_k$ are such that (2.2) is true. Then the matrix $\boldsymbol{A}(\boldsymbol{y}) = (P_i, P_j)_{\mathbf{y}}$ can be written as

$$\begin{bmatrix} P_1(\boldsymbol{x}_{\alpha_1}) & P_1(\boldsymbol{x}_{\alpha_2}) & \ldots & P_1(\boldsymbol{x}_{\alpha_k}) \\ P_2(\boldsymbol{x}_{\alpha_1}) & P_2(\boldsymbol{x}_{\alpha_2}) & \ldots & P_2(\boldsymbol{x}_{\alpha_k}) \\ \vdots & \vdots & \ddots & \vdots \\ P_m(\boldsymbol{x}_{\alpha_1}) & P_m(\boldsymbol{x}_{\alpha_2}) & \ldots & P_m(\boldsymbol{x}_{\alpha_k}) \end{bmatrix} * \begin{bmatrix} \mathcal{W}_{\alpha_1}(\boldsymbol{y}) & 0 & \ldots & 0 \\ 0 & \mathcal{W}_{\alpha_2}(\boldsymbol{y}) & \ldots & 0 \\ \vdots & \vdots & \ddots & \vdots \\ 0 & 0 & \ldots & \mathcal{W}_{\alpha_k}(\boldsymbol{y}) \end{bmatrix} *$$

$$* \begin{bmatrix} P_1(\boldsymbol{x}_{\alpha_1}) & P_2(\boldsymbol{x}_{\alpha_1}) & \ldots & P_m(\boldsymbol{x}_{\alpha_1}) \\ P_1(\boldsymbol{x}_{\alpha_2}) & P_2(\boldsymbol{x}_{\alpha_2}) & \ldots & P_m(\boldsymbol{x}_{\alpha_2}) \\ \vdots & \vdots & \ddots & \vdots \\ P_1(\boldsymbol{x}_{\alpha_k}) & P_2(\boldsymbol{x}_{\alpha_k}) & \ldots & P_m(\boldsymbol{x}_{\alpha_k}) \end{bmatrix} := \boldsymbol{F}\boldsymbol{W}\boldsymbol{F}^T$$

The rank of $\boldsymbol{F}$, and consequently of $\boldsymbol{A}$, will be at most equal to $k$, so, for $\boldsymbol{A}$ be positive definite, we must have $k \geq m$.

Now suppose that $\#\boldsymbol{P} = 1$ and, without loss of generality, that $P_1 = 1$. In this case the matrix $(P_k, P_l)_{\mathbf{y}}$ reduces to a single entry

$$\boldsymbol{A}(\boldsymbol{y}) = \sum_{j=1}^{k} \mathcal{W}_{\alpha_j}(\boldsymbol{y})$$

which is a positive number from the definition of the weight functions and the conditions of the theorem are also sufficient.

Let $\bar{\Omega} \subset \mathbb{R}^2, \boldsymbol{P} = \{1, x, y\}$, and $\boldsymbol{x}_{\alpha_a}, \boldsymbol{x}_{\alpha_b}, \boldsymbol{x}_{\alpha_c}$ be the three points not aligned. In this case the matrix $\boldsymbol{F}$ defined before reduces to

$$\boldsymbol{F} = \begin{bmatrix} 1 & 1 & \ldots & 1 \\ x_{\alpha_a} & x_{\alpha_b} & \ldots & x_{\alpha_c} \\ y_{\alpha_a} & y_{\alpha_b} & \ldots & y_{\alpha_c} \end{bmatrix}$$

The rows of $\boldsymbol{F}$ are linearly independent since

$$\begin{vmatrix} 1 & 1 & 1 \\ x_{\alpha_a} & x_{\alpha_b} & x_{\alpha_c} \\ y_{\alpha_a} & y_{\alpha_b} & y_{\alpha_c} \end{vmatrix} = 2 * \triangle$$

where $\triangle$ is the area of a triangle having the nodes $\boldsymbol{x}_{\alpha_a}, \boldsymbol{x}_{\alpha_b}, \boldsymbol{x}_{\alpha_c}$ as vertices. Thus the $rank(\boldsymbol{F}) = 3$ and $rank(\boldsymbol{F}^T) = 3$. Also $\boldsymbol{W}$ is positive definite since $\mathcal{W}_{\alpha_j}(\boldsymbol{y}) > 0$, $j = 1, \ldots, k$. These imply that $\boldsymbol{A}$ is positive-definite ∎

We are now in a position to define the signed partition of unity used in the $hp$ cloud method. The function $\varphi_\alpha$ associated to the ball $\omega_\alpha$ is defined by

$$\boxed{\varphi_\alpha(\boldsymbol{x}) := \boldsymbol{P}^T(\boldsymbol{x})\boldsymbol{A}^{-1}(\boldsymbol{x})\boldsymbol{B}_\alpha(\boldsymbol{x})} \tag{2.3}$$

where

- $A_{ij}(\boldsymbol{x}) := (P_i, P_j)_{\mathbf{x}}, \qquad P_i, P_j \in \boldsymbol{P}$
- $\boldsymbol{P}(\boldsymbol{x}) := \{P_1(\boldsymbol{x}), P_2(\boldsymbol{x}), \ldots, P_m(\boldsymbol{x})\}^T\ ,\ \exists\ P_j\ s.t.\ P_j(\boldsymbol{x}) \equiv 1$
- $\boldsymbol{B}_\alpha(\boldsymbol{x}) := \mathcal{W}_\alpha(\boldsymbol{x})\boldsymbol{P}(\boldsymbol{x}_\alpha)$

The next lemma and theorem will show that the definition of $\varphi_\alpha$ given in (2.3) satisfies the definition of a signed partition of unity.

**Lemma 2.4** *If $P_i$, $i = 1, \ldots, n, \in C^m(\Omega)$ and $\mathcal{W}_\alpha$, $\alpha = 1, \ldots, N, \in C^l(\Omega)$ then $\varphi_\alpha(\boldsymbol{x})$ as defined above $\in C^{min(m,l)}(\Omega)$.*

**Proof:**

Define

$$\boldsymbol{C}_\alpha(\boldsymbol{x}) := \boldsymbol{A}^{-1}(\boldsymbol{x})\boldsymbol{B}_\alpha(\boldsymbol{x})$$

then

$$\varphi_\alpha(\boldsymbol{x}) = \boldsymbol{P}^T(\boldsymbol{x})\boldsymbol{C}_\alpha(\boldsymbol{x})$$

and

$$\boldsymbol{A}(\boldsymbol{x})\boldsymbol{C}_\alpha(\boldsymbol{x}) = \boldsymbol{B}_\alpha(\boldsymbol{x})$$

Thus, using the Leibniz formula [1],

$$\begin{aligned}
D^\beta(\boldsymbol{A}\boldsymbol{C}_\alpha) &= \sum_{\gamma \leq \beta} \binom{\boldsymbol{\beta}}{\boldsymbol{\gamma}} D^\gamma \boldsymbol{A}\ D^{\beta-\gamma}\boldsymbol{C}_\alpha = D^\beta \boldsymbol{B}_\alpha \\
&= \boldsymbol{A}\ D^\beta \boldsymbol{C}_\alpha + \sum_{\substack{\gamma \leq \beta \\ \gamma \neq 0}} \binom{\boldsymbol{\beta}}{\boldsymbol{\gamma}} D^\gamma \boldsymbol{A}\ D^{\beta-\gamma}\boldsymbol{C}_\alpha \\
D^\beta \boldsymbol{C}_\alpha &= \boldsymbol{A}^{-1}[D^\beta \boldsymbol{B}_\alpha - \sum_{\substack{\gamma \leq \beta \\ \gamma \neq \boldsymbol{0}}} \binom{\boldsymbol{\beta}}{\boldsymbol{\gamma}} D^\gamma \boldsymbol{A}\ D^{\beta-\gamma}\boldsymbol{C}_\alpha]
\end{aligned}$$

The last expression makes sense since by hypothesis $\boldsymbol{A}^{-1}$ exists and by the assumption on the differentiability of $\mathcal{W}_\alpha$, $D^\beta \boldsymbol{B}_\alpha$ and $D^\beta \boldsymbol{A}$ also exists if $|\boldsymbol{\beta}| \leq l$. The lower order derivatives of $\boldsymbol{C}_\alpha$ that appear on the right hand side can be computed recursively using the above expression. So we conclude that $\boldsymbol{C}_\alpha \in C^l(\Omega)$ and the conclusion of the lemma is immediate ∎

**Theorem 2.5** *Let $1 \in \boldsymbol{P}$. Then the functions $\varphi_\alpha$ defined in (2.3) satisfy conditions 1) and 2) of a signed partition of unity. In addition, the $\varphi_\alpha$ are $\boldsymbol{P}$-reducible for the set $\boldsymbol{Q}_N$.*

**Proof:**

Let $P_l \in \boldsymbol{P}$. From the definition of $\varphi_\alpha$ given in (2.3)

$$\begin{aligned}
\sum_{\alpha=1}^{N} P_l(\boldsymbol{x}_\alpha)\varphi_\alpha(\boldsymbol{x}) &= \sum_{\alpha=1}^{N} P_l(\boldsymbol{x}_\alpha) \sum_{j,k=1}^{m} P_k(\boldsymbol{x}) A^{-1}_{kj}(\boldsymbol{x}) \mathcal{W}_\alpha(\boldsymbol{x}) P_j(\boldsymbol{x}_\alpha) \\
&= \sum_{j,k=1}^{m} \sum_{\alpha=1}^{N} P_l(\boldsymbol{x}_\alpha) P_j(\boldsymbol{x}_\alpha) \mathcal{W}_\alpha(\boldsymbol{x}) A^{-1}_{kj}(\boldsymbol{x}) P_k(\boldsymbol{x}) \\
&= \sum_{j,k=1}^{m} A_{lj}(\boldsymbol{x}) A^{-1}_{jk}(\boldsymbol{x}) P_k(\boldsymbol{x}) \\
&= P_l(\boldsymbol{x})
\end{aligned}$$

which shows that the $\varphi_\alpha$ are $\boldsymbol{P}$- reducible for the set $\boldsymbol{Q}_N$.

Since $1 \in \boldsymbol{P}$, the above gives

$$1 = \sum_{\alpha=1}^{N} 1(\boldsymbol{x}_\alpha)\varphi_\alpha(\boldsymbol{x}) = \sum_{\alpha=1}^{N} \varphi_\alpha(\boldsymbol{x})$$

Lemma 2.4 concludes the proof ∎

## 2.3 Where do the $\varphi'_\alpha s$ Come From ?

In the previous section, the signed partition of unity $\{\varphi_\alpha\}_{\alpha=1}^N$ was defined using an axiomatic approach. In this section the set of functions $\{\varphi_\alpha\}_{\alpha=1}^N$ is defined using a constructive approach. The strategy used here follows that of Moving Least Squares Methods (MLSM) and a more detailed account on the subject can be found in [14, 25, 44].

Suppose that a continuous function $u : \bar{\Omega} \to I\!R$, $\bar{\Omega} \subset I\!R^n, n = 1, 2$ or 3 is to be approximated and that its values $u_\alpha$ at the set of nodes $\boldsymbol{Q}_N$ are given. In the MLSM, we first construct at each point $\boldsymbol{y} \in \bar{\Omega}$ a local weighted least squares approximation, $L_{\mathbf{y}}u$, of $u$ using a set $\boldsymbol{P} = \{P_i\}_{i=1}^m$ of $m$ functions that satisfies the Assumption 2.1

$$(L_{\mathbf{y}}u)(\boldsymbol{x}) := \sum_{i=1}^{m} a_i(\boldsymbol{y}) P_i(\boldsymbol{x}) \qquad P_i \in \boldsymbol{P} \tag{2.4}$$

The coefficients $\boldsymbol{a}(\boldsymbol{y}) := \{a_i(\boldsymbol{y})\}_{i=1}^m$ are found by solving the following problem:

Find $\boldsymbol{a}^*(\boldsymbol{y}) \in I\!R^n$ such that $\forall\, \boldsymbol{a}(\boldsymbol{y}) \in I\!R^n$.

$$\begin{aligned} J(\boldsymbol{a}^*) &= (u - \sum_i^m a_i^* P_i, u - \sum_i^m a_i^* P_i)_{\mathbf{y}} \\ &\leq (u - \sum_i^m a_i P_i, u - \sum_i^m a_i P_i)_{\mathbf{y}} \end{aligned} \tag{2.5}$$

where $(.,.)_{\mathbf{y}}$ was defined in (2.1).

Inequality (2.5) implies that

$$(u - \sum_i^m a_i^* P_i, P_j)_{\mathbf{y}} = 0 \qquad j = 1, \ldots, m$$

Thus

$$\sum_i^m (P_i, P_j)_{\mathbf{y}} a_i^* = (u, P_j)_{\mathbf{y}} \qquad j = 1, \ldots, m$$

and

$$a_k^*(\boldsymbol{y}) = \sum_j^m A_{kj}^{-1} (u, P_j)_{\mathbf{y}}$$

where $A_{kj} := (P_k, P_j)_{\mathbf{y}}$. The local approximant of $u$, $L_{\mathbf{y}}u$, can be written as

$$\begin{aligned} (L_{\mathbf{y}}u)(\boldsymbol{x}) &= \sum_k^m a_k^*(\boldsymbol{y}) P_k(\boldsymbol{x}) \\ &= \sum_\alpha^N \sum_j^m \sum_k^m P_k(\boldsymbol{x}) A_{kj}^{-1}(\boldsymbol{y}) \mathcal{W}_\alpha(\boldsymbol{y}) P_j(\boldsymbol{x}_\alpha) u_\alpha \\ &:= \sum_\alpha^N \varphi_\alpha^{\mathbf{y}}(\boldsymbol{x}) u_\alpha \end{aligned}$$

where

$$\varphi_\alpha^{\mathbf{y}}(\boldsymbol{x}) = \sum_j^m \sum_k^m P_k(\boldsymbol{x}) A_{kj}^{-1}(\boldsymbol{y}) \mathcal{W}_\alpha(\boldsymbol{y}) P_j(\boldsymbol{x}_\alpha)$$

If $\boldsymbol{x} = \boldsymbol{y}$, we can drop the superscript $\boldsymbol{y}$ and define

$$\boxed{\varphi_\alpha(\boldsymbol{y}) = \sum_j^m \sum_k^m P_k(\boldsymbol{y}) A_{kj}^{-1}(\boldsymbol{y}) \mathcal{W}_\alpha(\boldsymbol{y}) P_j(\boldsymbol{x}_\alpha)}$$

which is precisely the definition given in (2.3).

## 2.4 The Families $\mathcal{F}_N^{k,p}$

The most important step in the *hp* cloud method is the construction of the family of functions $\mathcal{F}_N^{k,p}$ using the signed partition of unity $\{\varphi_\alpha\}_{\alpha=1}^N$ defined in the previous section. This class of functions can be constructed at a very low cost and has the important property that $\mathcal{P}_p \subset span\{\mathcal{F}_N^{k,p}\}$ where $\mathcal{P}_p$ denotes the space of polynomials of degree less or equal $p$. In this section we describe the construction of $\mathcal{F}_N^{k,p}$ and prove some theorems concerning some fundamental properties of these functions.

Let $\mathcal{L}_p$ denote the set of tensor product Legendre polynomials $L_{i,j,k}$ in $\mathbb{R}^3$

$$L_{ijk} = L_i(x_1)L_j(x_2)L_k(x_3), \qquad 0 \leq i,j,k \leq p$$

Other sets of complete polynomials can be used as well, e.g., the smallest set of complete polynomials $\Pi_p$. The set $\{\varphi_\alpha^k\}_{\alpha=1}^N$ will denote a signed partition of unity that is $\mathcal{L}_k$ - *reducible* for the set $\boldsymbol{Q}_N$, that is, given any element $L_{ijk} \in \mathcal{L}_k$ the following holds $\forall\ \boldsymbol{x} \in \bar{\Omega}$

$$L_{ijk}(\boldsymbol{x}) = \sum_{\alpha=1}^N L_{ijk}(\boldsymbol{x}_\alpha)\varphi_\alpha^k(\boldsymbol{x}) \tag{2.6}$$

The family of functions $\mathcal{F}_N^{k,p}$ is defined by

$$
\boxed{\begin{aligned}
\mathcal{F}_N^{k,p} \;=\; & \{\, \{\varphi_\alpha^k(\boldsymbol{x})\} \cup \{\varphi_\alpha^k L_{ijl}(\boldsymbol{x})\} : 1 \le \alpha \le N;\ 0 \le i,j,l \le p, \\
& i \text{ or } j \text{ or } l > k;\ \ p \ge k \,\}
\end{aligned}}
\tag{2.7}
$$

The idea behind the definition in (2.7) is to add, hierarchically, appropriate elements to the set $\{\varphi_\alpha^k\}_{\alpha=1}^N$ such that the resulting set can reproduce, in the sense of (2.6), polynomials of degree $p \ge k$. Because of property 2) of a signed partition of unity those elements are precisely the product of the functions $\varphi_\alpha^k$ with the elements from the set $\mathcal{L}_p$ that are missing from the set $\mathcal{L}_k$. Figures 2.2 and 2.3 illustrate the situation for the case $n = 2$, $k = 1$ and $p = 3$ when $\mathcal{L}_p$ is a set of tensor product polynomials in $\mathbb{R}^2$ and when $\mathcal{L}_p$ is equal to $\Pi_p(\mathbb{R}^2)$, respectively.

| | | $L_0(x_2)$ | $L_1(x_2)$ | $L_2(x_2)$ | $L_3(x_2)$ | $\dots$ |
|---|---|---|---|---|---|---|
| | $L_0(x_1)$ | $L_0L_0$ | $L_0L_1$ | $\underline{L_0L_2}$ | $\underline{L_0L_3}$ | $\dots$ |
| $k=1$ | $L_1(x_1)$ | $L_1L_0$ | $L_1L_1$ | $\underline{L_1L_2}$ | $\underline{L_1L_3}$ | $\dots$ |
| | $L_2(x_1)$ | $\underline{L_2L_0}$ | $\underline{L_2L_1}$ | $\underline{L_2L_2}$ | $\underline{L_2L_3}$ | $\dots$ |
| $p=3$ | $L_3(x_1)$ | $\underline{L_3L_0}$ | $\underline{L_3L_1}$ | $\underline{L_3L_2}$ | $\underline{L_3L_3}$ | $\dots$ |
| | $\vdots$ | $\vdots$ | $\vdots$ | $\vdots$ | $\vdots$ | $\ddots$ |

Figure 2.2: The elements used to build the family $\mathcal{F}_N^{k=1,p=3}$, when tensor product polynomials are used, are those underlined.

$$
\begin{array}{cc}
 & L_0L_0 \\
k=1 & L_1L_0 \ \ L_0L_1 \\
\hline
 & \underline{L_2L_0}\ \ \underline{L_1L_1}\ \ \underline{L_0L_2} \\
p=3 & \underline{L_3L_0}\ \ \underline{L_2L_1}\ \ \underline{L_1L_2}\ \ \underline{L_0L_3} \\
\hline
 & \vdots
\end{array}
$$

Figure 2.3: The elements used to build the family $\mathcal{F}_N^{k=1,p=3}$, when the sets $\Pi_{k=1}(\mathbb{R}^2)$ and $\Pi_{p=3}(\mathbb{R}^2)$ are used, are those underlined.

For consistent results, regardless of the scale of the problem, the *hp* cloud functions introduced in (2.7) are implemented using *h*-affine maps given by:

$$\mathbf{F}_\alpha : \widehat{\omega}_\alpha \rightarrow \omega_\alpha$$

$$\mathbf{F}_\alpha(\boldsymbol{\xi}) = h_\alpha \boldsymbol{\xi} + \boldsymbol{x}_\alpha, \qquad \boldsymbol{\xi} \in \widehat{\omega}_\alpha$$

where

$$\widehat{\omega}_\alpha := \{\boldsymbol{\xi} \in \mathbb{R}^n : \|\boldsymbol{\xi}\|_{\mathbb{R}^n} < 1\}$$

is a sphere of radius one and

$$\omega_\alpha := \{\boldsymbol{x} \in \mathbb{R}^n : \|\boldsymbol{x}_\alpha - \boldsymbol{x}\|_{\mathbb{R}^n} < h_\alpha\}$$

is the support of the function $\varphi_\alpha$.

The *hp* cloud function $\varphi_\alpha L_{ijl}(\boldsymbol{x})$ is implemented by

$$\varphi_\alpha L_{ijl}(\boldsymbol{x}) := \varphi_\alpha(\boldsymbol{x}) \widehat{L}_{ijl} \circ \mathbf{F}_\alpha^{-1}(\boldsymbol{x})$$

where $\widehat{L}_{ijl}(\boldsymbol{\xi})$ is a tensor product Legendre polynomial defined on $[-1,1]^n$.

The family $\mathcal{F}_N^{k,p}$ represents a generalization of some classes of functions used in diverse fields such as interpolation of functions [25, 44] and solution of boundary-value problems [28]. The Shephard functions [44] corresponds to the family

$$\mathcal{F}_N^{k=0,p=0} = \{\varphi_1^0, \varphi_2^0, \dots, \varphi_N^0\}$$

The approximation technique developed by Liszka (with the appropriate choice of the stars, see [14] for more details) [27, 28] corresponds to the family

$$\mathcal{F}_N^{k=2,p=2} = \{\varphi_1^2, \varphi_2^2, \dots, \varphi_N^2\}$$

The moving least squares method developed by [25] corresponds to the use of the families

$$\mathcal{F}_N^{k,p=k} = \{\varphi_1^k, \varphi_2^k, \dots, \varphi_N^k\}$$

This class of functions have also been used in the EFGM and DEM to solve boundary-value problems [5, 6, 40]. The class of functions used in the *hp* cloud method is a generalization of the above

$$\mathcal{F}_N^{k,p} = \left\{ \begin{array}{cccc} \varphi_1^k, & \varphi_2^k, & \dots, & \varphi_N^k \\ \varphi_1^k L_{s=1}, & \varphi_2^k L_{s=1}, & \dots, & \varphi_N^k L_{s=1}, \\ \varphi_1^k L_{s=2}, & \varphi_2^k L_{s=2}, & \dots, & \varphi_N^k L_{s=2}, \\ \vdots & \vdots & \ddots & \vdots \\ \varphi_1^k L_{s=M}, & \varphi_2^k L_{s=M}, & \dots, & \varphi_N^k L_{s=M} \end{array} \right\}$$

where

$$M = ((p+1)^n - (k+1)^n)$$

if tensor product polynomials are used in $I\!R^n$ and

$$M = \binom{p+n}{n} - \binom{k+n}{n}$$

if the sets $\Pi_k(I\!R^n)$ and $\Pi_p(I\!R^n)$ of complete polynomials are used.

We now prove two theorems that justify the use of the family $\mathcal{F}_N^{k,p}$ to approximate functions.

**Theorem 2.6** *The set $\mathcal{F}_N^{k,p}$ has the following properties:*

**i)** *If the set of moving least squares functions $\{\varphi_\alpha^k\}_{\alpha=1}^N$ is linearly independent in $I\!R^n$ then the set $\mathcal{F}_N^{k,p}$ is also a linearly independent set of functions in $I\!R^n$.*

**ii)** *dim $\mathcal{F}_N^{k,p} = N + N((p+1)^n - (k+1)^n)$ if tensor product polynomials are used.*

**iii)** *dim $\mathcal{F}_N^{k,p} = N + N\left(\binom{p+n}{n} - \binom{k+n}{n}\right)$ if the sets $\prod_k(I\!R^n)$ and $\prod_p(I\!R^n)$ of complete polynomials are used.*

*where $n$ is the dimension of the space.*

**Proof:**( for $n = 3$)

Suppose that

$$\begin{aligned}
\sum_{\alpha}^{N}\left(a_\alpha \varphi_\alpha^k(\boldsymbol{x}) + \sum_{\substack{0\le i,j,l\le p\\ i \text{ or } j \text{ or } l>k}} b_{\alpha ijl}\varphi_\alpha^k L_{ijl}(\boldsymbol{x})\right) &= 0\\
\sum_{\alpha}^{N}\varphi_\alpha^k(\boldsymbol{x})\left(a_\alpha + \sum_{\substack{0\le i,j,l\le p\\ i \text{ or } j \text{ or } l>k}} b_{\alpha ijl} L_{ijl}(\boldsymbol{x})\right) &= 0
\end{aligned}$$

Since $\{\varphi_\alpha^k\}_{\alpha=1}^N$ is a linearly independent set we must have

$$a_\alpha + \sum_{\substack{0\le i,j,l\le p\\ i \text{ or } j \text{ or } l>k}} b_{\alpha ijl} L_{ijl}(\boldsymbol{x}) = 0 \qquad \alpha = 1, \ldots, N$$

Since the set $\{L_{ijl}\}$ is a linearly independent set and there is no linear combination of the functions $L_{ijl}(\boldsymbol{x})$ that is equal to a constant, we must have

$$a_\alpha \equiv 0, \qquad b_{\alpha ijl} \equiv 0$$

■

**Theorem 2.7** $L_{ijl} \in span(\mathcal{F}_N^{k,p})$, *for* $0 \leq i, j, l \leq p$.

**Proof:**

If $L_{rst}$, $0 \leq r, s, t \leq p \in span(\mathcal{F}_N^{k,p})$ then $\exists\, a_\alpha$ and $b_{\alpha ijl}$ such that

$$L_{rst}(\boldsymbol{x}) = \sum_{\alpha}^{N} \left( a_\alpha \varphi_\alpha^k(\boldsymbol{x}) + \sum_{\substack{0 \leq i,j,l \leq p \\ i\ or\ j\ or\ l > k}} b_{\alpha ijl} \varphi_\alpha^k L_{ijl}(\boldsymbol{x}) \right)$$

If $r, s$ and $t \leq k$ then

$$a_\alpha = L_{rst}(\boldsymbol{x}_\alpha) \qquad \alpha = 1, \ldots, N$$

$$b_{\alpha ijl} \equiv 0$$

will work since the functions $\varphi_\alpha^k$ are $\mathcal{L}_k$ reducible.

If $r$ *or* $s$ *or* $t > k$ then take

$$a_\alpha \equiv 0$$

$$b_{\alpha ijl} = \begin{cases} 1 & \text{if i=r, j=s, l=t} \\ 0 & \text{otherwise} \end{cases} \qquad \alpha = 1, \ldots, N$$

then

$$\sum_{\alpha}^{N} \left( a_\alpha \varphi_\alpha^k(\boldsymbol{x}) + \sum_{\substack{0 \leq i,j,l \leq p \\ i\ or\ j\ or\ l > k}} b_{\alpha ijl} \varphi_\alpha^k L_{ijl}(\boldsymbol{x}) \right) =$$

$$\sum_{\alpha}^{N} \left( b_{\alpha rst} \varphi_\alpha^k L_{rst}(\boldsymbol{x}) \right) = L_{rst}(\boldsymbol{x}) \sum_{\alpha}^{N} \varphi_\alpha^k(\boldsymbol{x}) = L_{rst}(\boldsymbol{x})$$

■

### 2.4.1 Plot of The Cloud Shape Functions

The definition of the moving least squares functions give in (2.3) shows that, except for special cases, there is no closed form for these functions. The same applies for the cloud functions from the families $\mathcal{F}_N^{k,p}$ defined in (2.7). In this section the global shape functions $\Phi_I$ associated to a node $\boldsymbol{x}_I$ and corresponding to various choices of $k$ and $p$ are plotted for the one and two dimensional cases.

In the one dimensional case, the following parameters were used:

- $\Omega = [2.5, 7.5]$.
- Nodes: at $\boldsymbol{x}_I = 2.5 + I * 0.5,\ I = 0, \ldots, 10$.
- The set $\boldsymbol{P}$
  - ◦ $\boldsymbol{P} = \{1, x\}$ for the case $k = 1$.
  - ◦ $\boldsymbol{P} = \{1, x, x^2\}$ for the case $k = 2$.
  - ◦ $\boldsymbol{P} = \{1, x, x^2, x^3\}$ for the case $k = 3$.
- Weights

$$\mathcal{W}_I(\|\boldsymbol{y} - \boldsymbol{x}_I\|) = \begin{cases} \sqrt{4/\pi}\left(1.0 - \frac{\|\boldsymbol{y}-\boldsymbol{x}_I\|^2}{h_I^2}\right)^4 & if\ \|\boldsymbol{y} - \boldsymbol{x}_I\| < h_I \\ 0 & if\ \|\boldsymbol{y} - \boldsymbol{x}_I\| \geq h_I \end{cases}$$

  where $h_I = \alpha * d,\ d = 0.5,\ I = 0, \ldots, 10$ and the parameter $\alpha$ was chosen so that Assumption 2.1 is satisfied.

[40], [6] and [32] have used weighting functions built from the exponential function. We have, instead, chosen the above weighting function because it gives shape functions $\Phi_I$ that can be numerically integrated more precisely. This property may be important if the functions $\Phi_I$ are to be used in the Galerkin method.

Figure 2.4 [33] shows the functions $\varphi_5^{k=1}$ associated with node $\boldsymbol{x}_5$ for many values of the parameter $\alpha$ and linear $P_i$, that is, $k = p = 1$. It can be observed that as the support of the weight functions $\mathcal{W}_I$ approaches the support of a standard tent function, the function $\varphi_5^{k=1}$, built using the MLSM, approaches the shape of a tent function.

Figure 2.5 shows the function $\varphi_5^{k=1}$ for the case $\alpha = 3.0$ and linear $P_i$. Figure 2.6 shows all the functions $\varphi_N^{k=1}$, $N = 0, \ldots, 10$ for the case $\alpha = 3.0$.

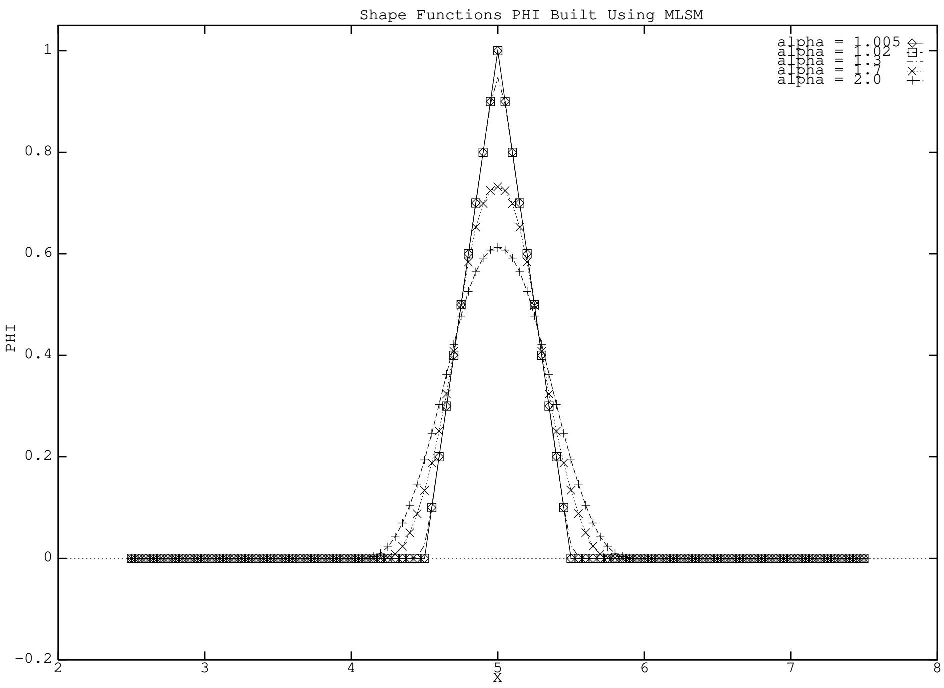


Figure 2.4: Functions $\varphi_5^{k=1}$ corresponding to $1.005 \leq \alpha \leq 2.0$ [33]

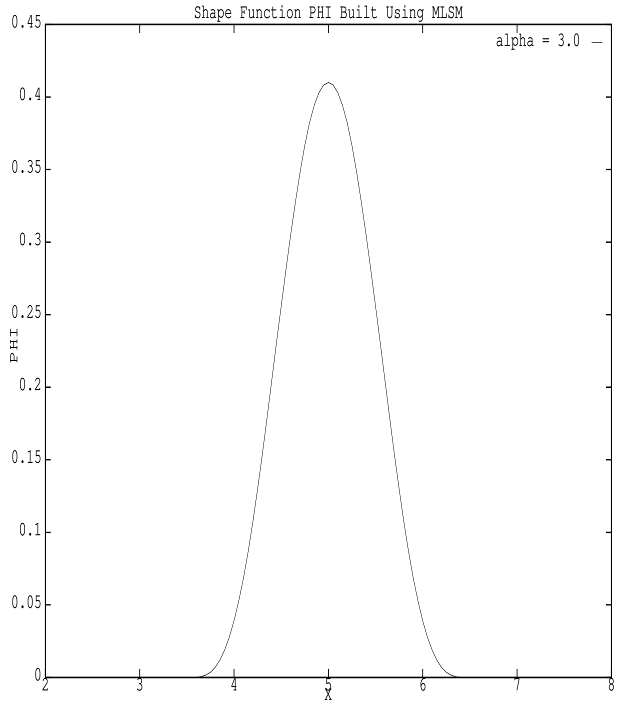


Figure 2.5: Function $\varphi_5^{k=1}$ corresponding to $\alpha = 3.0$

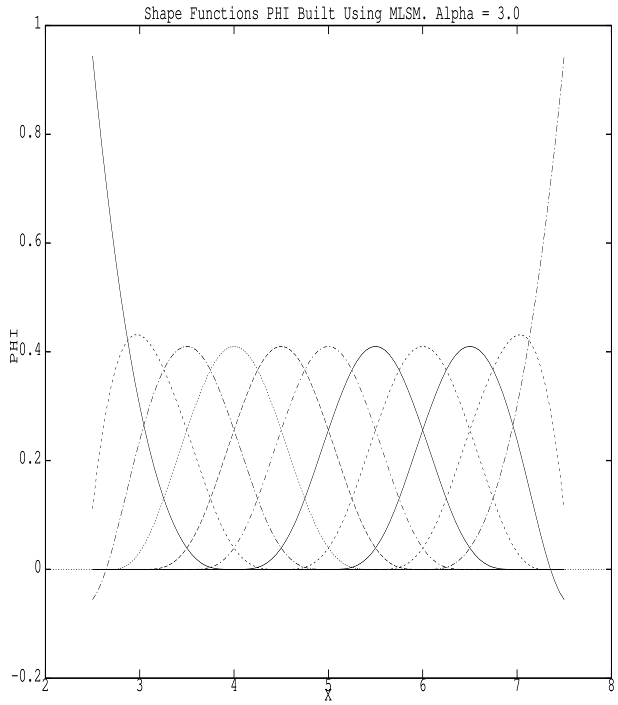


Figure 2.6: All Functions $\varphi_N^{k=1}$ corresponding to $\alpha = 3.0$

Note that none of the functions have value 1.0 at the nodes and that at any node there might be more than one function that is nonzero.

Figures 2.7 and 2.8 show the function associated with node $\boldsymbol{x}_5$ when using the sets $\boldsymbol{P} = \{1, x, x^2\}$ and $\boldsymbol{P} = \{1, x, x^2, x^3\}$, respectively. Note that the size of the support of the functions have to be increased when the dimension of the set $\boldsymbol{P}$ increases in order Assumption 2.1 is satisfied.

For the two dimensional case the node arrangement shown in Figure 2.9 was used. Figure 2.9 also shows a representation of the open covering $\mathcal{T}_N$. The balls $\omega_I$ are indeed circles in the two dimensional case but were graphically represented in Figure 2.9 using polygonals. In all two dimensional plots the domain $\Omega$ was either the square $[-1, 1] \times [-1, 1]$ or the square $[0, 1] \times [0, 1]$. The set $\boldsymbol{P}$, used to build the MLS functions $\varphi^k$, was composed of tensor product of one dimensional polynomials. The families $\mathcal{F}_N^{k,p}$ were also build using tensor product polynomials as defined in (2.7).

The following algorithm was developed and implemented to guarantee that Assumption 2.1 was satisfied when the degree, $k$, of the MLS functions was equal to 0 or 1. For $k \geq 2$ the algorithm guarantees that the necessary

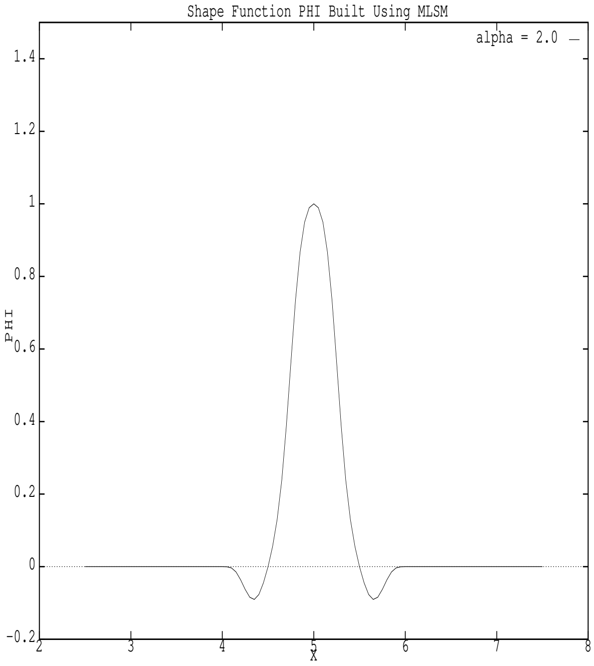


Figure 2.7: Function $\varphi_5^{k=2}$ corresponding to $\alpha = 2.0$

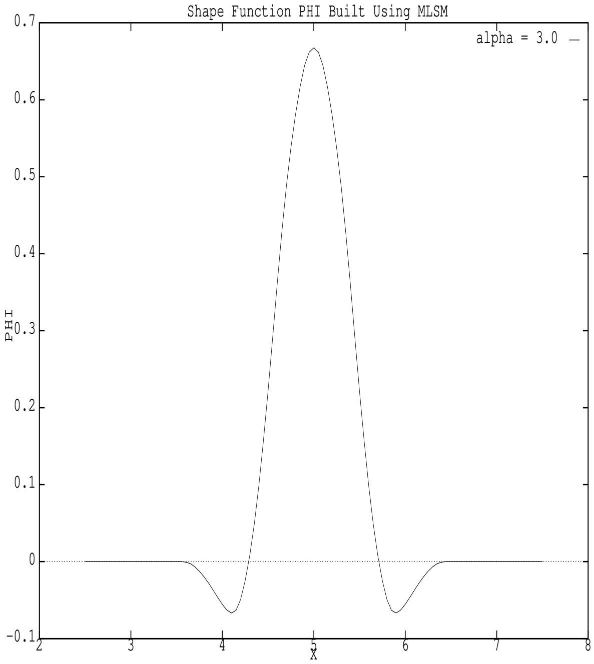


Figure 2.8: Function $\varphi_5^{k=3}$ corresponding to $\alpha = 3.0$

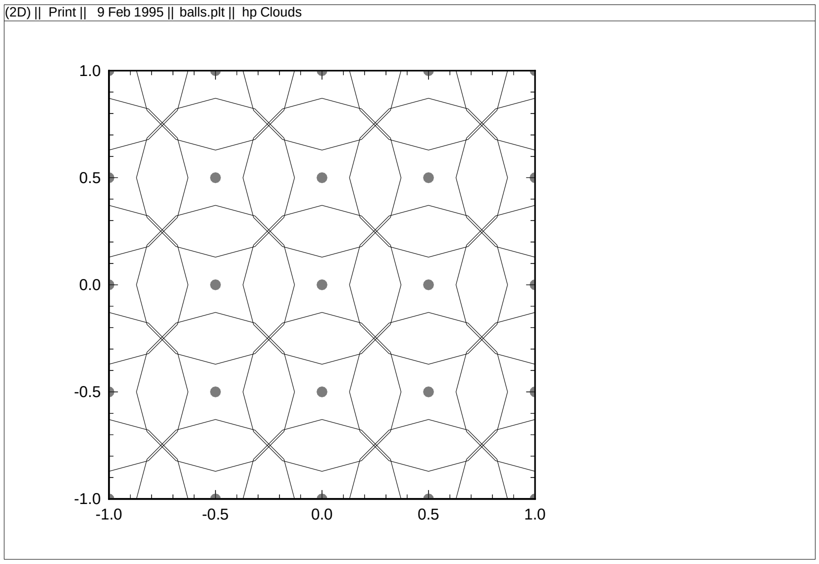


Figure 2.9: Node Arrangement and Support of Functions.

conditions for the satisfaction of Assumption 2.1 are met. In next sections we show that in the *hp* cloud method there is no advantage in using $k > 0$ which justify the use of the following algorithm in practical computations.

*For all balls* $\omega_\alpha$ *set* $h_\alpha = 0$

*For all points* $\boldsymbol{\xi}_k \in Q$ *do:*

- *Build a list List of all nodes that fall within a searching square centered at* $\boldsymbol{\xi}_k$ *and with sides equal to* $2 * R$, $R =$ *upper bound for* $h_\alpha$. *If dim(List)* $<$ *dim*$(\boldsymbol{P})$ *increase the size of the searching square and try again.*
- *Build a list Dist with the distance of the nodes List to the point* $\boldsymbol{\xi}_k$.
- *Sort the list Dist.*
- *Enforces that* $\boldsymbol{\xi}_k$ *belongs to the support of the dim*$(\boldsymbol{P})$ *closest nodes from List. This is accomplished using the list Dist and the values of* $h_\alpha$.
- *If* $k = 1$ *check if there are at least 3 nodes not aligned in the list of the dim*$(\boldsymbol{P})$ *closest nodes. If necessary enforces that* $\boldsymbol{\xi}_k$ *belongs also to the support of other nodes in the list List.*

*End do.*

In the above $Q$ is the index set of all points in $\Omega$ that we want to build a cloud function using moving least squares functions $\varphi^k$.

The above algorithm requires an efficient means of determining which nodes fall within a specified region of the domain. This same kind of problems appears in the smoothed particle hydrodynamics method [45]. Swegle and colleagues [45] developed a very efficient algorithm to perform this kind of search. The algorithm can be used in any dimension and the total execution time of the algorithm is of order $\dim(Q)\log(N)$ where $N$ is the total number of nodes. We have used this algorithm in our implementation.

Figure 2.10 shows one function from the family $\mathcal{F}_N^{k=0,p}$ associated to a node that lays on the boundary of the domain. Note that the function is not defined outside of $\Omega$. Figure 2.11 shows another function from the same family. Figure 2.12 shows the corresponding function from the family $\mathcal{F}_N^{k=1,p}$. Note that visually the two functions do not differ very much.

Figures 2.13, 2.14 and 2.15 show the functions $\varphi_N^{k=1}y^2$, $\varphi_N^{k=1}y^3$ and $\varphi_N^{k=1}xy^2$ from the family $\mathcal{F}_N^{k=1,p=3}$, respectively.

Figure 2.16 shows one function from the family $\mathcal{F}_N^{k=2,p}$ associated to a node that lays at a corner point of the domain $\Omega$. Figure 2.17 shows a function, from the same family, associated to a node at the boundary of $\Omega$.

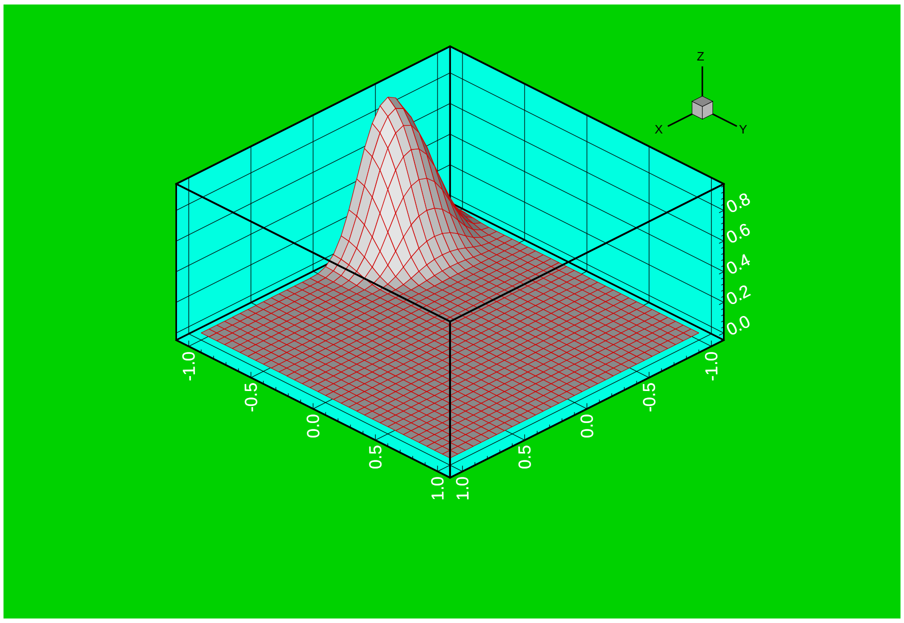


Figure 2.10: 2-D function: $\varphi_N^{k=0}$ from the family $\mathcal{F}_N^{k=0,p}$

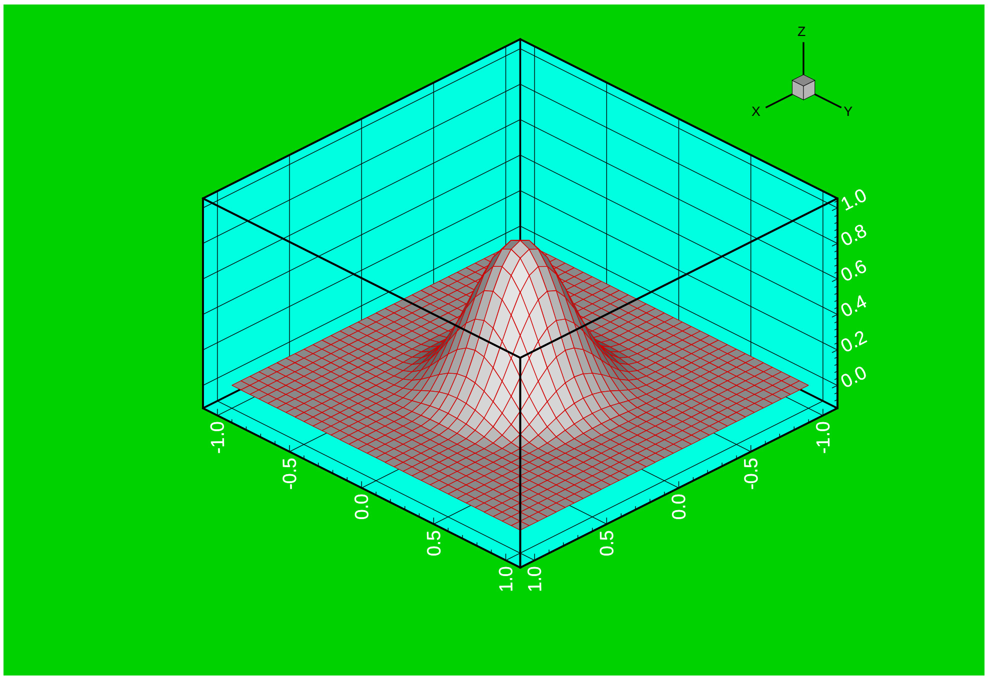


Figure 2.11: 2-D function: $\varphi_N^{k=0}$ from the family $\mathcal{F}_N^{k=0,p}$

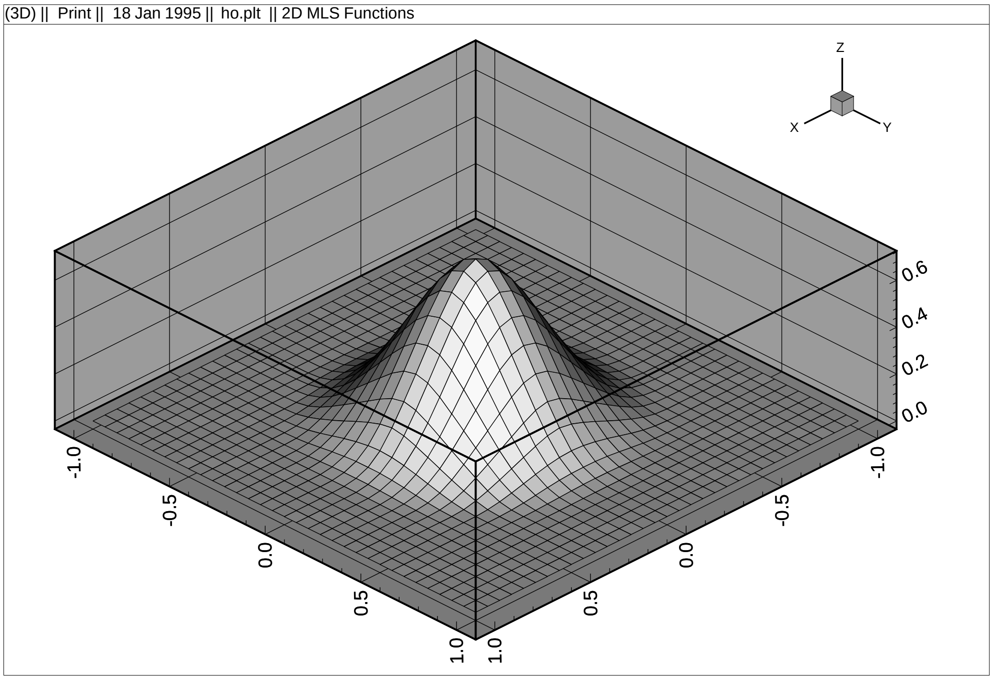


Figure 2.12: 2-D function: $\varphi_N^{k=1}$ from the family $\mathcal{F}_N^{k=1,p}$

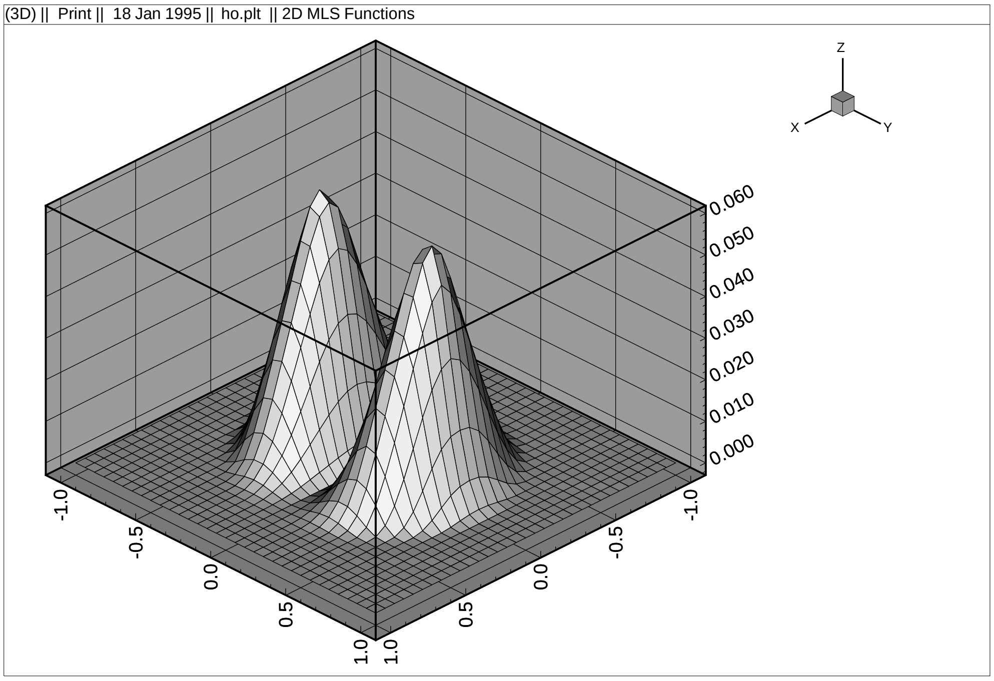


Figure 2.13: 2-D function: $\varphi_N^{k=1} y^2$ from the family $\mathcal{F}_N^{k=1,p=3}$

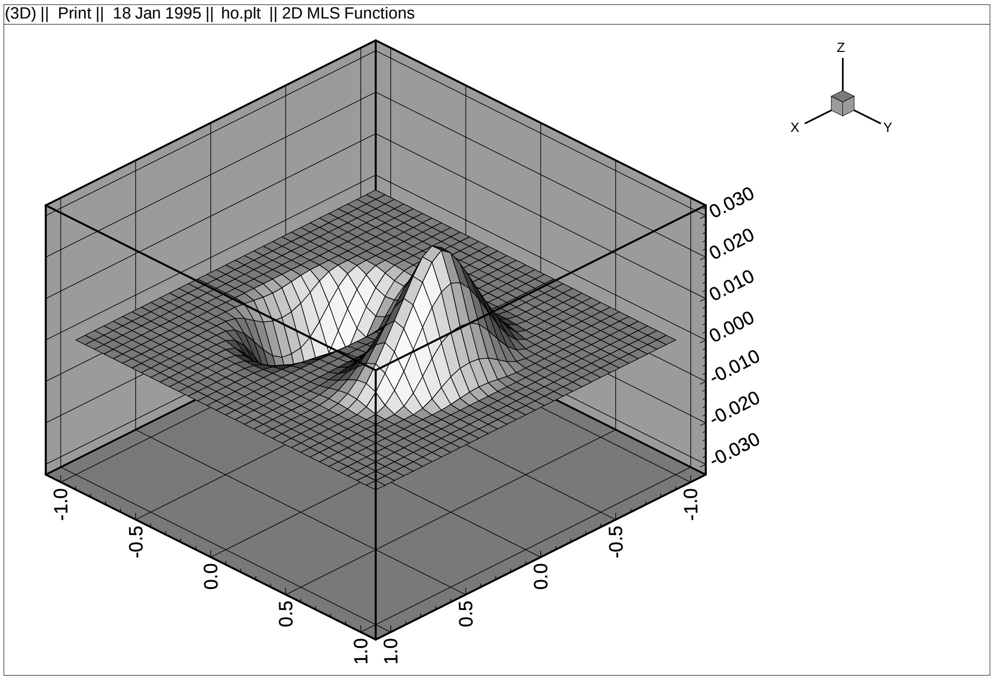


Figure 2.14: 2-D function: $\varphi_N^{k=1} y^3$ from the family $\mathcal{F}_N^{k=1,p=3}$

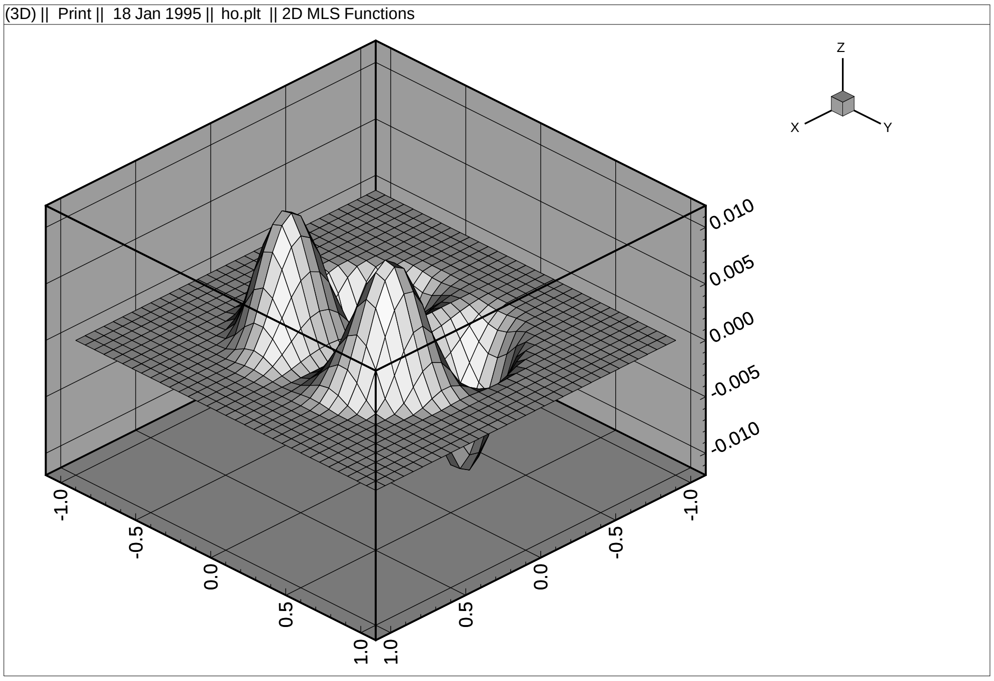


Figure 2.15: 2-D function: $\varphi_N^{k=1} xy^2$ from the family $\mathcal{F}_N^{k=1,p=3}$

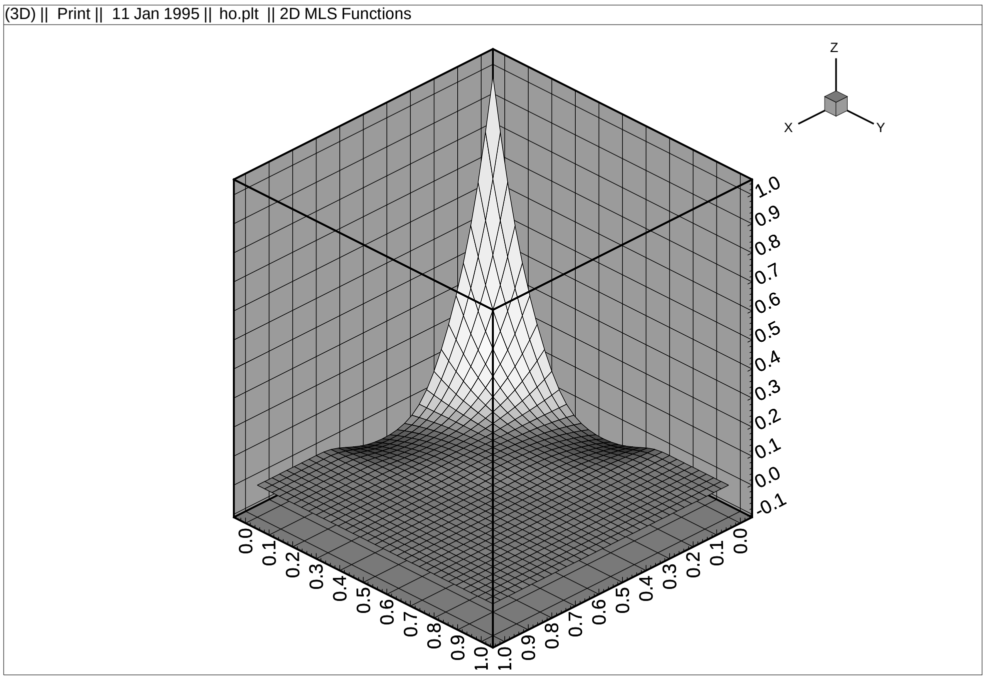


Figure 2.16: 2-D function: $\varphi_N^{k=2}$ from the family $\mathcal{F}_N^{k=2,p}$

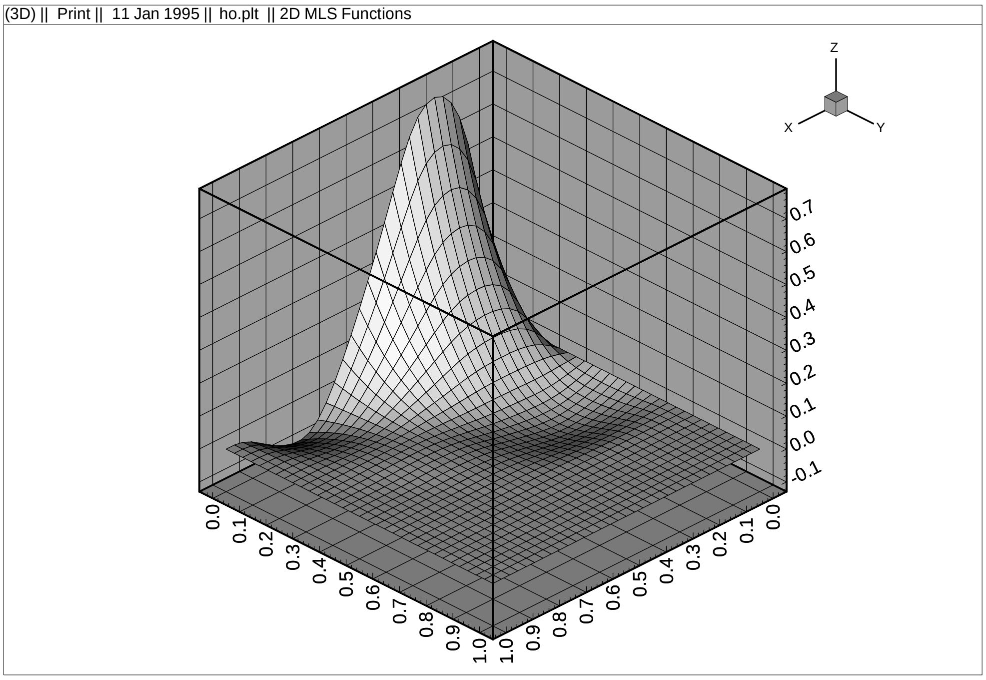


Figure 2.17: 2-D function: $\varphi_N^{k=2}$ from the family $\mathcal{F}_N^{k=2,p}$

# 3 Approximation Theory for the $hp$ Cloud Method—$h$ Convergence

## 3.1 Introduction

In this section, we consider the problem of determining estimates in appropriate norms and semi-norms of the difference $(u - u_h)$, where $u$ is a function that belongs to a given Sobolev space $\boldsymbol{X}$ and $u_{hp}$ is an approximation of $u$ built using $hp$ cloud methods and belonging to a subspace $\boldsymbol{X}^{hp}$ of $\boldsymbol{X}$.

The strategy used to derive the local estimates follows closely that of [10, 41] in the context of finite element methods. The approach used to derive the global estimates follows [4, 35, 36].

## 3.2 Preliminaries

We define a *ball* in $\mathbb{R}^n$ as the triple $(\overline{\omega}_\alpha, \boldsymbol{\Xi}_\alpha^{hp}, \mathbb{L}_\alpha^2)$ where:

**(i)** $\overline{\omega}_\alpha$ is a closed subset of $\mathbb{R}^n$ given by

$$\overline{\omega}_\alpha := \overline{\{\boldsymbol{y} \in \mathbb{R}^n : \|\boldsymbol{x}_\alpha - \boldsymbol{y}\|_{\mathbb{R}^n} < h_\alpha\}} \qquad \boldsymbol{x}_\alpha \in \bar{\Omega}$$

**(ii)** $\boldsymbol{\Xi}_\alpha^{hp}$ is a space of real-valued functions defined over the set $\overline{\omega}_\alpha$ and given by

$$\boldsymbol{\Xi}_\alpha^{hp} := span\left\{\mathcal{F}_N^{k,p}|_{\omega_\alpha}\right\} \equiv span\left\{\Phi_j^\alpha\right\}_{j\in I}$$

where $\mathcal{F}_N^{k,p}$ is the set of global cloud functions defined in previous section, $\Phi_j^\alpha \in$ basis of $\boldsymbol{\Xi}_\alpha^{hp}$, that is, it is a shape function, and $I$ is an index set.

**(iii)** $\mathbb{L}_\alpha^2$ is a set of linearly independent linear forms $a_l$, where $l \in I$, defined over the space $\boldsymbol{\Xi}_\alpha^{hp}$ and given by

$$a_l(v) := \sum_{j\in I}(M_{lj}^\alpha)^{-1}(v, \Phi_j^\alpha)_{L^2(\omega_\alpha)} \tag{3.1}$$

where

- $v \in \boldsymbol{\Xi}_\alpha^{hp}$
- $M_{lj}^\alpha = (\Phi_l^\alpha, \Phi_j^\alpha)_{L^2(\omega_\alpha)} = \int_{\omega_\alpha} \Phi_l^\alpha \Phi_j^\alpha d\boldsymbol{x}$

The functionals $a_l$ will be denoted by degrees of freedom.

Given a ball $(\overline{\omega}_\alpha, \boldsymbol{\Xi}_\alpha^{hp}, \mathbb{L}_\alpha^2)$, and given a function $v : \overline{\omega}_\alpha \to \mathbb{R}$ sufficiently smooth so that the degrees of freedom $a_l$, $l \in I$, are well defined, we let

$$\Pi_\alpha^2 v := \sum_{i\in I} a_i(v)\Phi_i^\alpha \tag{3.2}$$

denote the $L^2$–approximation of the function $v$ over the domain $\overline{\omega}_\alpha$.

**Proposition 3.1** *It follows from the definition of the operator $\Pi_\alpha^2$ that over the space $\boldsymbol{\Xi}_\alpha^{hp} \subset dom\Pi_\alpha^2$, the operator reduces to the identity operator, i.e.,*

$$\forall\, g \in \boldsymbol{\Xi}_\alpha^{hp}, \qquad \Pi_\alpha^2 g = g$$

*that is, $\Pi_\alpha^2$ is a projection operator.*

**Proof:**

Let $g \in \boldsymbol{\Xi}_\alpha^{hp}$, then we can write

$$g = \sum_{m\in I} \alpha_m \Phi_m^\alpha$$

then

$$\begin{aligned} a_l(g) &= \sum_{j\in I} (\Phi_l^\alpha, \Phi_j^\alpha)^{-1}_{L^2(\omega_\alpha)} (\Phi_j^\alpha, \sum_{m\in I} \alpha_m \Phi_m^\alpha)_{L^2(\omega_\alpha)} \\ &= \sum_{m\in I} \alpha_m \underbrace{\sum_{j\in I} (\Phi_l^\alpha, \Phi_j^\alpha)^{-1}_{L^2(\omega_\alpha)} (\Phi_j^\alpha, \Phi_m^\alpha)_{L^2(\omega_\alpha)}}_{\delta_{lm}} = \alpha_l \end{aligned}$$

Thus

$$\Pi_\alpha^2 g = \sum_{l\in I} a_l(g)\Phi_l^\alpha = \sum_{l\in I} \alpha_l \Phi_l^\alpha = g$$

∎

**Corollary 3.2** *The projection operator $\Pi_\alpha^2$ preservers polynomials of degree $\leq p$; that is*

$$\Pi_\alpha^2 t = t \qquad \forall\, t \in \mathcal{P}_p(\omega_\alpha)$$

*where $p$ is the parameter that appears in the definition of the space $\boldsymbol{\Xi}_\alpha^{hp}$.*

**Proof:**

It follows immediately from previous proposition and Theorem 2.7. ∎

We will say that the open set $\omega_\alpha$ is $h$-affine equivalent to the open set $\widehat{\omega}_\alpha$ if there is an affine mapping between $\omega_\alpha$ and $\widehat{\omega}_\alpha$ of the form

$$\mathbf{F}_\alpha : \widehat{\omega}_\alpha \to \omega_\alpha$$

$$\mathbf{F}_\alpha(\boldsymbol{\xi}) = h_\alpha \boldsymbol{\xi} + \mathbf{C}, \qquad \boldsymbol{\xi} \in \widehat{\omega}_\alpha$$

and $\forall\, \boldsymbol{y} \in \omega_\alpha$, $\exists\, \boldsymbol{\xi} \in \widehat{\omega}_\alpha$ such that $\boldsymbol{y} = \mathbf{F}_\alpha(\boldsymbol{\xi})$.

Once we have established the bijection

$$\boldsymbol{\xi} \in \widehat{\omega}_\alpha \to \boldsymbol{y} = \mathbf{F}_\alpha(\boldsymbol{\xi}) \in \omega_\alpha$$

between the points of the sets $\widehat{\omega}_\alpha$ and $\omega_\alpha$, it is natural to associate the space

$$\widehat{\boldsymbol{\Xi}}_\alpha^{hp} := \left\{ \widehat{\Phi}_i^\alpha : \widehat{\omega}_\alpha \to \mathbb{R} |\ \widehat{\Phi}_i^\alpha = \Phi_i^\alpha \circ \mathbf{F}_\alpha(\boldsymbol{\xi}),\ \Phi_i^\alpha \in \boldsymbol{\Xi}_\alpha^{hp} \right\}$$

with the space $\boldsymbol{\Xi}_\alpha^{hp}$.

With these definitions in mind we are in a position to give the following definition:

Two balls $(\overline{\omega}_\alpha, \boldsymbol{\Xi}_\alpha^{hp}, \mathbb{L}_\alpha^2)$ and $(\widehat{\omega}_\alpha, \widehat{\boldsymbol{\Xi}}_\alpha^{hp}, \widehat{\mathbb{L}}_\alpha^2)$ are said to be *h-affine equivalents* if there is an $h$-affine mapping $\mathbf{F}_\alpha$ between $\omega_\alpha$ and $\widehat{\omega}_\alpha$ such that the following relations hold:

**(i)** $\omega_\alpha = \mathbf{F}_\alpha(\widehat{\omega}_\alpha)$

**(ii)** $\widehat{\boldsymbol{\Xi}}_\alpha^{hp} = \left\{ \widehat{\Phi}_i^\alpha : \widehat{\omega}_\alpha \to I\!R |\; \widehat{\Phi}_i^\alpha = \Phi_i^\alpha \circ \mathbf{F}_\alpha(\boldsymbol{\xi}),\; \Phi_i^\alpha \in \boldsymbol{\Xi}_\alpha^{hp} \right\}$

**(iii)** $\hat{a}_l = a_l \qquad l \in I$

where the functionals $a_l$ were defined in (3.1) and $\hat{a}_l$ are given by

$$\hat{a}_l(\hat{v}) = \sum_{j\in I} (\widehat{M}_{lj}^\alpha)^{-1} (\hat{v}, \widehat{\Phi}_j^\alpha)_{L^2(\widehat{\omega}_\alpha)} \tag{3.3}$$

where

- $\hat{v} \in \widehat{\boldsymbol{\Xi}}_\alpha^{hp}$
- $\widehat{M}_{lj}^\alpha = (\widehat{\Phi}_l^\alpha, \widehat{\Phi}_j^\alpha)_{L^2(\widehat{\omega}_\alpha)}$

**Theorem 3.3** *Let $(\widehat{\omega}_\alpha, \widehat{\boldsymbol{\Xi}}_\alpha^{hp}, \widehat{I\!L}_\alpha^2)$ and $(\overline{\omega}_\alpha, \boldsymbol{\Xi}_\alpha^{hp}, I\!L_\alpha^2)$ be two h-affine equivalent balls with degrees of freedom in the form (3.1). Then if $\widehat{\Phi}_i^\alpha, i \in I$, are the basis functions of the ball $\widehat{\omega}_\alpha$, the functions $\Phi_i^\alpha, i \in I$, are the basis functions of the ball $\omega_\alpha$, the projection operators $\Pi_\alpha^2$ and $\widehat{\Pi}_\alpha^2$ are such that*

$$\widehat{\Pi_\alpha^2 v} = \widehat{\Pi}_\alpha^2 \hat{v}$$

*for any functions $\hat{v} \in dom \widehat{\Pi}_\alpha^2$ and $v \in dom \Pi_\alpha^2$ associated in the correspondence*

$$\hat{v} \in dom \widehat{\Pi}_\alpha^2 \to v = \hat{v} \circ \mathbf{F}^{-1} \in dom \Pi_\alpha^2$$

**Proof:**

The $L^2$–approximation operator $\Pi_\alpha^2$ is of the form

$$\Pi_\alpha^2 v = \sum_{k\in I} a_k(v) \Phi_i^\alpha$$

where

$$a_k(v) = \sum_{j\in I} (\Phi_k^\alpha, \Phi_j^\alpha)_{L^2(\omega_\alpha)}^{-1} (v, \Phi_j^\alpha)_{L^2(\omega_\alpha)}$$

$$\begin{aligned}
(\Phi_k^\alpha, \Phi_j^\alpha)_{L^2(\omega_\alpha)} &= \int_{\omega_\alpha} \Phi_k^\alpha(\boldsymbol{y}) \Phi_j^\alpha(\boldsymbol{y}) d\boldsymbol{y} = h^n \int_{\widehat{\omega}_\alpha} \widehat{\Phi}_k^\alpha(\boldsymbol{\xi}) \widehat{\Phi}_j^\alpha(\boldsymbol{\xi}) d\boldsymbol{\xi} \\
&= h^n (\widehat{\Phi}_k^\alpha, \widehat{\Phi}_j^\alpha)_{L^2(\widehat{\omega}_\alpha)}
\end{aligned}$$

$$
\begin{aligned}
(v, \Phi_j^\alpha)_{L^2(\omega_\alpha)} &= \int_{\omega_\alpha} v(\boldsymbol{y}) \Phi_j^\alpha(\boldsymbol{y}) d\boldsymbol{y} = h^n \int_{\widehat{\omega}_\alpha} \hat{v}(\boldsymbol{\xi}) \widehat{\Phi}_j^\alpha(\boldsymbol{\xi}) d\boldsymbol{\xi} \\
&= h^n (\hat{v}, \widehat{\Phi}_j^\alpha)_{L^2(\widehat{\omega}_\alpha)}
\end{aligned}
$$

Thus

$$
\begin{aligned}
a_k(v) &= \sum_{j \in I} \frac{1}{h^n} (\widehat{\Phi}_k^\alpha, \widehat{\Phi}_j^\alpha)^{-1}_{L^2(\widehat{\omega}_\alpha)} h^n (\hat{v}, \widehat{\Phi}_j^\alpha)_{L^2(\widehat{\omega}_\alpha)} \\
&= \hat{a}_k(\hat{v})
\end{aligned}
$$

Then

$$
\begin{aligned}
(\Pi_\alpha^2 v)(\boldsymbol{y}) &= \sum_{k \in I} a_k(v) \Phi_k^\alpha(\boldsymbol{y}) = \sum_{k \in I} \hat{a}_k(\hat{v}) \Phi_k^\alpha(\boldsymbol{y}) \\
(\widehat{\Pi_\alpha^2 v})(\boldsymbol{\xi}) &= (\Pi_\alpha^2 v) \circ \mathbf{F}_\alpha(\boldsymbol{\xi}) = \sum_{k \in I} \hat{a}_k(\hat{v}) \Phi_k^\alpha \circ \mathbf{F}_\alpha(\boldsymbol{\xi}) \\
&= \sum_{k \in I} \hat{a}_k(\hat{v}) \widehat{\Phi}_k^\alpha(\boldsymbol{\xi}) = \widehat{\Pi}_\alpha^2 \hat{v}(\boldsymbol{\xi})
\end{aligned}
$$

∎

The next theorem will be useful later on.

**Theorem 3.4** *[41] Let $W^{p+1,r}(\Omega) \hookrightarrow W^{m,s}(\Omega)$ and let $\Pi \in \mathcal{L}(W^{p+1,r}(\Omega), W^{m,s}(\Omega))$ be a linear continuous operator from $W^{p+1,r}(\Omega)$ onto $W^{m,s}(\Omega)$ which preserves polynomials of degree $\leq p$; that is*

$$
\Pi t = t \qquad \forall \; t \in \mathcal{P}_p(\Omega)
$$

*Then there exists a constant $C = C(\Omega)$ such that for every $v \in W^{p+1,r}(\Omega)$*

$$
|v - \Pi v|_{m,s,\Omega} \leq C(\Omega) \| I - \Pi \|_{\mathcal{L}(W^{p+1,r}(\Omega), W^{m,s}(\Omega))} |v|_{p+1,r,\Omega}
$$

**Proof:** See [41] ∎

**Theorem 3.5** *Let $\omega_\alpha$ and $\widehat{\omega}_\alpha$ be two h-affine equivalent open sets in $\mathbb{R}^n$. If a function $v \in W^{m,s}(\omega_\alpha)$ for some integer $m \geq 0$ and some number $s \geq 1$, the function $\hat{v} = v \circ \mathbf{F}_\alpha$ belongs to the space $W^{m,s}(\widehat{\omega}_\alpha)$, and, in addition, $\forall \; v \in W^{m,s}(\omega_\alpha)$ the following holds*

$$
|\hat{v}|_{m,s,\widehat{\omega}_\alpha} = \mathrm{h}_\alpha^{m - \frac{n}{s}} |v|_{m,s,\omega_\alpha}
$$

*where $h_\alpha$ is the parameter appearing in the h-affine mapping* $\mathbf{F}_\alpha(\boldsymbol{\xi}) = h_\alpha\boldsymbol{\xi} + \mathbf{C},\ \boldsymbol{\xi} \in \widehat{\omega}_\alpha$

*Analogously one has* $\forall\ \hat{v} \in W^{m,s}(\widehat{\omega}_\alpha)$

$$|v|_{m,s,\omega_\alpha} = \mathrm{h}_\alpha^{-m+\frac{n}{s}} |\hat{v}|_{m,s,\widehat{\omega}_\alpha}$$

**Proof:**

$$|\hat{v}|^s_{m,s,\widehat{\omega}_\alpha} = \int_{\widehat{\omega}_\alpha} \sum_{|\boldsymbol{\beta}|=m} |D^{\boldsymbol{\beta}}\hat{v}(\boldsymbol{\xi})|^s d\boldsymbol{\xi}$$

$$\frac{\partial \hat{v}}{\partial \xi_m}(\boldsymbol{\xi}) = \frac{\partial v}{\partial y_k}\frac{\partial y_k}{\partial \xi_m} = \frac{\partial v}{\partial y_k}\delta_{km} h_\alpha = h_\alpha \frac{\partial v}{\partial y_m}$$

Thus

$$\frac{\partial^l \hat{v}}{\partial \xi_m^l} = h_\alpha^l \frac{\partial^l v}{\partial y_m^l}$$

$$\frac{\partial^{\boldsymbol{\beta}} \hat{v}}{\partial \boldsymbol{\xi}^{\boldsymbol{\beta}}} = \frac{\partial^{\beta_1} v}{\partial \xi_1^{\beta_1}}\frac{\partial^{\beta_2} v}{\partial \xi_2^{\beta_2}} \cdots \frac{\partial^{\beta_n} v}{\partial \xi_n^{\beta_n}} = h_\alpha^{\beta_1} h_\alpha^{\beta_2} \ldots h_\alpha^{\beta_n} \frac{\partial^{\beta_1} v}{\partial y_1^{\beta_1}}\frac{\partial^{\beta_2} v}{\partial y_2^{\beta_2}} \cdots \frac{\partial^{\beta_n} v}{\partial y_n^{\beta_n}}$$

So,

$$D^{\boldsymbol{\beta}}\hat{v}(\boldsymbol{\xi}) = h_\alpha^{|\boldsymbol{\beta}|} D^{\boldsymbol{\beta}} v(\boldsymbol{y})$$

$$\begin{aligned}
|\hat{v}|^s_{m,s,\widehat{\omega}_\alpha} &= \int_{\widehat{\omega}_\alpha} \sum_{|\boldsymbol{\beta}|=m} |D^{\boldsymbol{\beta}}\hat{v}(\boldsymbol{\xi})|^s d\boldsymbol{\xi} \\
&= \int_{\omega_\alpha} \sum_{|\boldsymbol{\beta}|=m} |h_\alpha^{|\boldsymbol{\beta}|} D^{\boldsymbol{\beta}} v(\boldsymbol{y})|^s \frac{1}{h_\alpha^n} d\boldsymbol{y} \\
&= \frac{h_\alpha^{ms}}{h_\alpha^n} \int_{\omega_\alpha} \sum_{|\boldsymbol{\beta}|=m} |D^{\boldsymbol{\beta}} v(\boldsymbol{y})|^s d\boldsymbol{y} \\
&= \frac{h_\alpha^{ms}}{h_\alpha^n} |v|^s_{m,s,\omega_\alpha}
\end{aligned}$$

Thus

$$|\hat{v}|_{m,s,\widehat{\omega}_\alpha} = h_\alpha^{m-\frac{n}{s}} |v|_{m,s,\omega_\alpha} \rightarrow \hat{v} \in W^{m,s}(\widehat{\omega}_\alpha)$$

The second assertion is proved in an analogous manner ∎

We are now in a position to prove an important property of polynomial preserving operators. The key idea is to go from an open set $\Omega$ to an $h$-affine equivalent $\widehat{\Omega}$ and then go back to $\Omega$. The following theorem is restricted to the case of $h$-affine maps, which is the kind of mappings we are interested on. A more general version of it can be found in [10].

**Theorem 3.6** *For some integers $p \geq 0$ and $m \geq 0$ and some numbers $r, s \in [1, \infty]$, let $W^{p+1,r}(\widehat{\Omega})$ and $W^{m,s}(\widehat{\Omega})$ be Sobolev spaces satisfying the inclusion*

$$W^{p+1,r}(\widehat{\Omega}) \hookrightarrow W^{m,s}(\widehat{\Omega})$$

*and let $\widehat{\Pi} \in \mathcal{L}(W^{p+1,r}(\widehat{\Omega}), W^{m,s}(\widehat{\Omega}))$ be a mapping such that*

$$\forall\ \hat{t} \in \mathcal{P}_p(\widehat{\Omega}) \qquad \widehat{\Pi}\hat{t} = \hat{t}$$

*For any open set $\Omega$ which is h-affine equivalent to $\widehat{\Omega}$, let the mapping $\Pi_\Omega v$ be defined by*

$$(\widehat{\Pi_\Omega v}) = \widehat{\Pi}\hat{v} \tag{3.4}$$

*for all functions $\hat{v} \in W^{p+1,r}(\widehat{\Omega})$ and $v \in W^{m,s}(\widehat{\Omega})$ in the correspondence*

$$\hat{v} = v \circ \mathbf{F}(\boldsymbol{\xi}) \qquad\qquad \mathbf{F}(\boldsymbol{\xi}) = h\boldsymbol{\xi} + \mathbf{C} \tag{3.5}$$

*Then there exists a constant $C(\widehat{\Pi}, \widehat{\Omega})$ such that, for all h-affine equivalent sets $\Omega$, $\forall\ v \in W^{p+1,r}(\Omega)$*

$$\boxed{|v - \Pi_\Omega v|_{m,s,\Omega} \leq C(\widehat{\Pi}, \widehat{\Omega}) h^{p+1-m+\frac{n}{s}-\frac{n}{r}} |v|_{p+1,r,\Omega}} \tag{3.6}$$

*with $h$ given by (3.5).*

**Proof:** Theorem 3.5 gives that

$$|v - \Pi_\Omega v|_{m,s,\Omega} = h^{-m+\frac{n}{s}} |\widehat{v - \Pi_\Omega v}|_{m,s,\widehat{\Omega}}$$

It follows from relation (3.4) that

$$\widehat{v - \Pi_\Omega v} = \hat{v} - \widehat{\Pi}\hat{v}$$

Therefore, using Theorem 3.4 we get

$$\begin{aligned}
|\widehat{v - \Pi_\Omega v}|_{m,s,\widehat{\Omega}} &= |\hat{v} - \widehat{\Pi}_\Omega \hat{v}|_{m,s,\widehat{\Omega}} \\
&\leq C(\widehat{\Omega}) \left\| I - \widehat{\Pi} \right\|_{\mathcal{L}(W^{p+1,r}(\widehat{\Omega}), W^{m,s}(\widehat{\Omega}))} |\hat{v}|_{p+1,r,\widehat{\Omega}} \\
&= C(\widehat{\Pi}, \widehat{\Omega}) |\hat{v}|_{p+1,r,\widehat{\Omega}}
\end{aligned}$$

But by Theorem 3.5 we have

$$|\hat{v}|_{p+1,r,\widehat{\Omega}} = h^{p+1-\frac{n}{r}} |v|_{p+1,r,\Omega}$$

Thus

$$|v - \Pi_\Omega v|_{m,s,\Omega} \leq C(\widehat{\Pi}, \widehat{\Omega}) h^{p+1-m+\frac{n}{s}-\frac{n}{r}} |v|_{p+1,r,\Omega}$$

∎

## 3.3 Estimates of the Approximation Error $|v - \Pi^2_\alpha v|_{m,s,\omega_\alpha}$ for a Ball

By specializing Theorem 3.6 to balls, we obtain estimates of the approximation error $|v - \Pi^2_\alpha v|_{m,s,\omega_\alpha}$. Before that we need a few more results.

**Theorem 3.7** *The linear mapping $\widehat{\Pi}^2_\alpha : W^{p+1,r}(\widehat{\omega}_\alpha) \to W^{m,s}(\widehat{\omega}_\alpha)$ (the space $\widehat{\boldsymbol{\Xi}}^{hp}_\alpha$ is contained in the space $W^{m,s}(\widehat{\omega}_\alpha)$) is continuous.*

**Proof:**

Let $\hat{v} \in W^{p+1,r}(\widehat{\omega}_\alpha)$ then, from the definition of $\widehat{\Pi}^2_\alpha$

$$(\widehat{\Pi}^2_\alpha \hat{v})(\boldsymbol{\xi}) = \sum_{l\in I} \hat{a}_l(\hat{v})\widehat{\Phi}^\alpha_l(\boldsymbol{\xi})$$

where

$$\hat{a}_l(\hat{v}) = \sum_{j\in I}(\widehat{M}_{lj})^{-1}(\hat{v}, \widehat{\Phi}^\alpha_j)_{L^2(\widehat{\omega}_\alpha)}$$

and

$$\widehat{M}^\alpha_{lj} = (\widehat{\Phi}^\alpha_l, \widehat{\Phi}^\alpha_j)_{L^2(\widehat{\omega}_\alpha)}$$

Thus

$$\begin{aligned}
\left\|\widehat{\Pi}^2_\alpha \hat{v}\right\|_{m,s,\widehat{\omega}_\alpha} &\le \sum_{l\in I} |\hat{a}_l| \left\|\widehat{\Phi}^\alpha_l\right\|_{m,s,\widehat{\omega}_\alpha} \\
&= \sum_{l\in I} |\sum_{j\in I}(\widehat{M}_{lj})^{-1}(\hat{v}, \widehat{\Phi}^\alpha_j)_{L^2(\widehat{\omega}_\alpha)}| \left\|\widehat{\Phi}^\alpha_l\right\|_{m,s,\widehat{\omega}_\alpha} \\
&\le \sum_{l\in I}\sum_{j\in I} |\widehat{M}_{lj}|^{-1}| \left\|\widehat{\Phi}^\alpha_j\right\|_{L^2(\widehat{\omega}_\alpha)} \left\|\widehat{\Phi}^\alpha_l\right\|_{m,s,\widehat{\omega}_\alpha} \|\hat{v}\|_{L^2(\widehat{\omega}_\alpha)} \\
&\le \left(\sum_{l\in I}\sum_{j\in I} |\widehat{M}_{lj}|^{-1}| \left\|\widehat{\Phi}^\alpha_j\right\|_{L^2(\widehat{\omega}_\alpha)} \left\|\widehat{\Phi}^\alpha_l\right\|_{m,s,\widehat{\omega}_\alpha}\right) \|\hat{v}\|_{p+1,r,\widehat{\omega}_\alpha}
\end{aligned}$$

Assume, without loss of generality, that the functions $\Phi^\alpha_l$, $l \in I$, have been orthonormalized with respect to the inner product $(.,.)_{L^2(\widehat{\omega}_\alpha)}$. This implies that

$$\widehat{M}_{lj} = \delta_{lj} = (\widehat{M}_{lj})^{-1}$$

and

$$\sum_{l\in I}\sum_{j\in I} |\widehat{M}^{-1}_{lj}| = \sum_{l\in I}\sum_{j\in I} \delta_{lj} = dim(\widehat{\boldsymbol{\Xi}}^{hp}_\alpha)$$

This leads us to an interesting observation: If we use only the family $\mathcal{F}_n^{k,p=k}$, that is, only the moving least squares functions $\varphi_I$'s, the dimension of the space $\widehat{\boldsymbol{\Xi}}_\alpha^{hp}$ is independent of $k$ (the degree of the polynomial that the functions $\varphi_I$ can reproduce). By the other hand, if we use the family $\mathcal{F}_n^{k,p}$, $p > k$, the dimension of the space $\widehat{\boldsymbol{\Xi}}_\alpha^{hp}$ will increase as we increase $p$ and keep $k$ fixed. Thus we can write

$$\sum_{l\in I}\sum_{j\in I}|\widehat{M}_{lj}^{-1}| \leq C(p)$$

note that $C$ is independent of $k$.

Collecting everything we get

$$\left\|\widehat{\Pi}_\alpha^2 \hat{v}\right\|_{m,s,\widehat{\omega}_\alpha} \leq C(\widehat{\Omega}, p, \widehat{\Pi}_\alpha^2)\,\|\hat{v}\|_{p+1,r,\widehat{\omega}_\alpha}$$

∎

**Theorem 3.8** *Let $(\widehat{\omega}_\alpha, \widehat{\boldsymbol{\Xi}}_\alpha^{hp}, \widehat{\mathbb{L}}_\alpha^2)$ be a ball with $\widehat{\boldsymbol{\Xi}}_\alpha^{hp}$ and $\widehat{\mathbb{L}}_\alpha^2$ defined as before. Suppose that the following holds for some integers $m \geq 0$, $p \geq 0$ and for some numbers $r, s \in [1,\infty]$*

$$W^{p+1,r}(\widehat{\omega}_\alpha) \hookrightarrow W^{m,s}(\widehat{\omega}_\alpha)$$

$$\mathcal{P}_p(\widehat{\omega}_\alpha) \subset \widehat{\boldsymbol{\Xi}}_\alpha^{hp} \subset W^{m,s}(\widehat{\omega}_\alpha)$$

*Then there exists a constant $C(\widehat{\omega}_\alpha, \widehat{\boldsymbol{\Xi}}_\alpha^{hp}(p), \widehat{\mathbb{L}}_\alpha^2)$ such that, for the h-affine equivalent ball $(\omega_\alpha, \boldsymbol{\Xi}_\alpha^{hp}(p), \mathbb{L}_\alpha^2)$ and all functions $v \in W^{p+1,r}(\omega_\alpha)$*

$$\boxed{|v - \Pi_\alpha^2 v|_{m,s,\omega_\alpha} \leq C(\widehat{\omega}_\alpha, \widehat{\boldsymbol{\Xi}}_\alpha^{hp}(p), \widehat{\mathbb{L}}_\alpha^2) h_\alpha^{p+1-m+\frac{n}{s}-\frac{n}{r}} |v|_{p+1,r,\omega_\alpha}} \qquad (3.7)$$

*where $h_\alpha$ is the parameter that appears in the h-affine mapping between $\widehat{\omega}_\alpha$ and $\omega_\alpha$.*

**Proof:** By Corollary 3.2 we have that

$$\forall\, \hat{t} \in \mathcal{P}_p(\widehat{\omega}_\alpha) \qquad \widehat{\Pi}_\alpha^2 \hat{t} = \hat{t}$$

Also, by Theorem 3.7 we have that

$$\widehat{\Pi}_\alpha^2 \in \mathcal{L}(W^{p+1,r}(\widehat{\omega}_\alpha), W^{m,s}(\widehat{\omega}_\alpha))$$

Since the $\Pi^2_\alpha$ and $\hat{\Pi}^2_\alpha$ projection operators are related through the correspondence

$$\widehat{\Pi^2_\alpha v} = \hat{\Pi}^2_\alpha \hat{v}$$

for any functions $v \in dom\Pi^2_\alpha$ and $\hat{v} \in dom\hat{\Pi}^2_\alpha$ (cf. Theorem 3.3), we may apply Theorem 3.6, and inequality (3.7) is just a re-statement of inequality (3.6) in the present case ∎

Note that:

**(i)** The rate of convergence given by (3.7) does not depend on the polynomial degree that the moving least squares functions can reproduce, but only on the degree that the functions $\Phi^\alpha_i$ can reproduce. That is, the rate given by the $h$-refinement using the family $\mathcal{F}^{k_1,p}_N$ is the same as the rate using the family $\mathcal{F}^{k_2,p}_N$. This is in agreement with our numerical experiments of Section 4.

**(ii)** The constant that appears in the inequality (3.7) does not depend on the polynomial degree that the moving least squares functions can reproduce, but only on the degree that the functions $\Phi^\alpha_i$ can reproduce. This indicates that $p$-refinement using only moving least squares functions will probably not decrease the approximation error. Again, this is in agreement with our numerical experiments of Section 4.

**(iii)** There is no aspect ratio effect in the inequality (3.7), unlike in the finite element method. This phenomena has been reported by Belytschko and colleagues in the element free Galerkin method [5, 6] which is a special case of the $hp$ cloud method.

## 3.4 Global Estimates

In this section we present an estimate of the difference $(u - u_{hp})$, where $u \in H^l(\Omega)$, $l \geq 1$, and $u_{hp}$ is an approximation of $u$ built using $hp$ cloud methods and belonging to a subspace $\boldsymbol{X}^{hp}$ of $H^1(\Omega)$. The approach used to derive the estimate follows that of Babuška and Rheinboldt [4] and of Melenk [35, 36].

The proofs are given for the case where the partition of unity $\{\varphi_\alpha\}^N_{\alpha=1}$ is built using only the constant 1, that is, the case $k = 0$ in the definition given by (2.7). This does not represent a limitation in practice since the numerical experiments of Section 4 show that the case $k = 0$ is indeed the best choice for the $hp$ cloud method.

Let $\widetilde{\boldsymbol{X}}_{\alpha}^{hp}(\omega_{\alpha}^{h})$ denote a two parameter family of spaces defined by

$$\widetilde{\boldsymbol{X}}_{\alpha}^{hp}(\omega_{\alpha}^{h}) := span \left\{ \widehat{L}_i \circ \boldsymbol{F}_{\alpha}^{-1} \right\}_{i=1}^{D(n,p)}$$

The mapping $\boldsymbol{F}_{\alpha}$ is the $h$-affine mapping defined before and the basis functions $\widehat{L}_i$ are chosen such that the following conditions are satisfied:

$$\widehat{L}_1(\boldsymbol{x}) \equiv 1$$

$$\mathcal{P}_p(\omega_{\alpha}) \subset \widetilde{\boldsymbol{X}}_{\alpha}^{hp}(\omega_{\alpha}^{h})$$

$D(n,p)$ depends on the choice of the set $\{\widehat{L}_i\}$. If, for example, $\widehat{L}_i$ are tensor product polynomials in $\mathbb{R}^n$ then

$$D(n,p) = (p+1)^n$$

The restriction of the elements of $\widetilde{\boldsymbol{X}}_{\alpha}^{hp}$ to $(\Omega \cap \omega_{\alpha}^{h})$ will be denoted by $\boldsymbol{X}_{\alpha}^{hp}$.

**Definition 3.9** *Let $\Omega \subset \mathbb{R}^n$ be an open set and $\mathcal{T}_{N(h)} = \{\omega_{\alpha}^{h}\}_{\alpha=1}^{N(h)}$, $h > 0$, be a one parameter family of open coverings of $\Omega$ where*

$$\max_{\alpha=1,\ldots,N(h)} h_{\alpha} \leq h$$

*and $h_{\alpha}$ is the radius of the ball $\omega_{\alpha}^{h}$. The family $\mathcal{T}_{N(h)}$ is said to satisfy the overlapping condition if $\exists\ \rho \in \mathbb{N}$ such that $\forall\ h > 0$ and $\forall\ \boldsymbol{x} \in \Omega$*

$$card\{\alpha \ :\ \boldsymbol{x} \in \omega_{\alpha}^{h}\} \leq \rho$$

We associate to the family of open coverings $\mathcal{T}_{N(h)}$ *a family of signed partitions of unity* $\{\varphi_{\alpha}^{h}\}_{\alpha=1}^{N(h)}$ built using only the constant 1 (k=0). The index $h$ is used to emphasize that $\{\varphi_{\alpha}^{h}\}_{\alpha=1}^{N(h)}$ is an element of a family of signed partitions of unity.

**Assumption 3.10** *The family of signed partitions of unity $\{\varphi_{\alpha}^{h}\}_{\alpha=1}^{N(h)}$ satisfy the following additional conditions:*

**1)** $\left\|\varphi_{\alpha}^{h}\right\|_{L^{\infty}(\Omega)} \leq C_{\infty}$

**2)** $\left\|\nabla\varphi_\alpha^h\right\|_{L^\infty(\Omega)} \leq \frac{C_G}{h_\alpha}$

*for some* $C_\infty,\ C_G > 0$ *independent of* $h$.

**Definition 3.11** *Let* $\boldsymbol{X}_\alpha^{hp} \subset H^1(\Omega\cap\omega_\alpha^h)$ *be the two parameter family of spaces defined above. The space* $\boldsymbol{X}^{hp}$ *is defined by*

$$\boldsymbol{X}^{hp} := \left\{ u_{hp} = \sum_{\alpha=1}^{N(h)} \varphi_\alpha^h u_\alpha^{hp} \ :\ u_\alpha^{hp} \in \boldsymbol{X}_\alpha^{hp} \right\}$$

**Lemma 3.12** $\boldsymbol{X}^{hp} = span\left\{\mathcal{F}_{N(h)}^{k=0,p}\right\}$.

**Proof:**

From the definition of $\boldsymbol{X}^{hp}$ we have that

$$\begin{aligned} u_{hp} &= \sum_{\alpha=1}^{N(h)} \varphi_\alpha^h u_\alpha^{hp} \\ &= \sum_{\alpha=1}^{N(h)} \sum_{i=1}^{D(n,p)} a_{i\alpha}\varphi_\alpha^h(\boldsymbol{x})\widehat{L}_i\left(\frac{\boldsymbol{x}-\boldsymbol{x}_\alpha}{h_\alpha}\right) \qquad \forall\ u_{hp} \in \boldsymbol{X}^{hp} \end{aligned}$$

where $\widehat{L}_1 \equiv 1$.

Consequently

$$\begin{aligned} \boldsymbol{X}^{hp} &= span\left\{ \begin{array}{cccc} \varphi_1^h 1, & \varphi_2^h 1, & \cdots, & \varphi_{N(h)}^h 1, \\ \varphi_1^h\widehat{L}_2\left(\frac{\boldsymbol{x}-\boldsymbol{x}_1}{h_1}\right), & \varphi_2^h\widehat{L}_2\left(\frac{\boldsymbol{x}-\boldsymbol{x}_2}{h_2}\right), & \cdots, & \varphi_{N(h)}^h\widehat{L}_2\left(\frac{\boldsymbol{x}-\boldsymbol{x}_{N(h)}}{h_{N(h)}}\right), \\ \varphi_1^h\widehat{L}_3\left(\frac{\boldsymbol{x}-\boldsymbol{x}_1}{h_1}\right), & \varphi_2^h\widehat{L}_3\left(\frac{\boldsymbol{x}-\boldsymbol{x}_2}{h_2}\right), & \cdots, & \varphi_{N(h)}^h\widehat{L}_3\left(\frac{\boldsymbol{x}-\boldsymbol{x}_{N(h)}}{h_{N(h)}}\right), \\ \vdots & \vdots & \ddots & \vdots \\ \varphi_1^h\widehat{L}_D\left(\frac{\boldsymbol{x}-\boldsymbol{x}_1}{h_1}\right), & \varphi_2^h\widehat{L}_D\left(\frac{\boldsymbol{x}-\boldsymbol{x}_2}{h_2}\right), & \cdots, & \varphi_{N(h)}^h\widehat{L}_D\left(\frac{\boldsymbol{x}-\boldsymbol{x}_{N(h)}}{h_{N(h)}}\right) \end{array} \right\} \\ &= span\left\{\mathcal{F}_{N(h)}^{k=0,p}\right\} \end{aligned}$$

■

**Theorem 3.13** *[35, 36] Let* $\Omega,\ \mathcal{T}_{N(h)} = \{\omega_\alpha^h\}_{\alpha=1}^{N(h)},\ \{\varphi_\alpha^h\}_{\alpha=1}^{N(h)}$ *and* $\boldsymbol{X}_\alpha^{hp}$ *be as defined above. Let* $u \in H^l(\Omega)$, $l \geq 1$, *and suppose that for fixed* $h$ *and* $p$

*the function $u$ can be approximated locally by functions in $\boldsymbol{X}_\alpha^{hp}$, i.e., for each $\alpha$ $\exists$ $u_\alpha^{hp} \in \boldsymbol{X}_\alpha^{hp}$ such that*

$$\begin{aligned}
\left\| u - u_\alpha^{hp} \right\|_{L^2(\Omega\cap\omega_\alpha^h)} &\leq C_1(\alpha, h, p) \left\| u \right\|_{H^l(\Omega\cap\omega_\alpha^h)} \\
|u - u_\alpha^{hp}|_{H^1(\Omega\cap\omega_\alpha^h)} &\leq C_2(\alpha, h, p) \left\| u \right\|_{H^l(\Omega\cap\omega_\alpha^h)}
\end{aligned}$$

*Then $\exists$ $u_{hp} \in \boldsymbol{X}^{hp}$ such that*

$$\begin{aligned}
\left\| u - u_{hp} \right\|_{L^2(\Omega)} &\leq \rho C_\infty \max_{\alpha=1,\ldots,N(h)} C_1(\alpha, h, p) \left\| u \right\|_{H^l(\Omega)}, \\
|u - u_{hp}|_{H^1(\Omega)} &\leq \sqrt{2}\rho \max_{\alpha=1,\ldots,N(h)} \left( \frac{C_G C_1(\alpha, h, p)}{h_\alpha} + C_\infty C_2(\alpha, h, p) \right) \left\| u \right\|_{H^l(\Omega)}
\end{aligned}$$

*where the constants $C_\infty$ and $C_G$ where defined in Assumption 3.10.*

**Proof:** [35, 36]

From the definition of the space $\boldsymbol{X}^{hp}$ and the fact that $\{\varphi_\alpha^h\}_{\alpha=1}^{N(h)}$ form a partition of unity we have

$$\left\| u - u_{hp} \right\|_{L^2(\Omega)}^2 = \left\| \sum_{\alpha=1}^{N(h)} \varphi_\alpha^h (u - u_\alpha^{hp}) \right\|_{L^2(\Omega)}^2 = \int_\Omega \left| \sum_{\alpha=1}^{N(h)} \varphi_\alpha^h (u - u_\alpha^{hp}) \right|^2 d\Omega$$

Using Schwarz inequality and the fact that for a fixed $\boldsymbol{x} \in \Omega$ there is no more than $\rho$ non zero terms in the above sum, we get

$$\begin{aligned}
\int_\Omega \left| \sum_{\alpha=1}^{N(h)} \varphi_\alpha^h (u - u_\alpha^{hp}) \right|^2 d\Omega &\leq \rho \int_\Omega \sum_{\alpha=1}^{N(h)} \left| \varphi_\alpha^h (u - u_\alpha^{hp}) \right|^2 d\Omega \\
&\leq \rho C_\infty^2 \sum_{\alpha=1}^{N(h)} \int_{\Omega\cap\omega_\alpha^h} \left| u - u_\alpha^{hp} \right|^2 d\Omega \\
&\leq \rho C_\infty^2 \sum_{\alpha=1}^{N(h)} C_1^2(\alpha, h, p) \left\| u \right\|_{H^l(\Omega\cap\omega_\alpha^h)}^2 \\
&\leq \rho C_\infty^2 \max_{\alpha=1,\ldots,N(h)} C_1^2(\alpha, h, p) \rho \left\| u \right\|_{H^l(\Omega)}^2
\end{aligned}$$

The semi-norm estimate follows as above

$$\begin{aligned}
\left\| \nabla(u - u_{hp}) \right\|_{L^2(\Omega)}^2 &= \left\| \sum_{\alpha=1}^{N(h)} [\nabla\varphi_\alpha^h (u - u_\alpha^{hp})] + \sum_{\alpha=1}^{N(h)} [\varphi_\alpha^h \nabla(u - u_\alpha^{hp})] \right\|_{L^2(\Omega)}^2 \\
&= \int_\Omega \left| \sum_{\alpha=1}^{N(h)} [\nabla\varphi_\alpha^h (u - u_\alpha^{hp})] + \sum_{\alpha=1}^{N(h)} [\varphi_\alpha^h \nabla(u - u_\alpha^{hp})] \right|^2 d\Omega
\end{aligned}$$

Using Schwarz inequality for the two terms sum and then again for each of the other sums and the fact that for a fixed $\boldsymbol{x} \in \Omega$ there is no more than $\rho$ non zero terms in these sums, we get

$$
\begin{aligned}
&\int_\Omega \left| \sum_{\alpha=1}^{N(h)} [\nabla \varphi_\alpha^h (u - u_\alpha^{hp})] + \sum_{\alpha=1}^{N(h)} [\varphi_\alpha^h \nabla (u - u_\alpha^{hp})] \right|^2 d\Omega \\
\leq\ & \int_\Omega \left\{ 2 \left| \sum_{\alpha=1}^{N(h)} [\nabla \varphi_\alpha^h (u - u_\alpha^{hp})] \right|^2 + 2 \left| \sum_{\alpha=1}^{N(h)} [\varphi_\alpha^h \nabla (u - u_\alpha^{hp})] \right|^2 \right\} d\Omega \\
\leq\ & 2 \int_\Omega \left\{ \rho \sum_{\alpha=1}^{N(h)} \left| \nabla \varphi_\alpha^h (u - u_\alpha^{hp}) \right|^2 + \rho \sum_{\alpha=1}^{N(h)} \left| \varphi_\alpha^h \nabla (u - u_\alpha^{hp}) \right|^2 \right\} d\Omega \\
\leq\ & 2 \frac{C_G^2}{h_\alpha^2} \rho \sum_{\alpha=1}^{N(h)} \int_{\Omega \cap \omega_\alpha^h} \left| (u - u_\alpha^{hp}) \right|^2 d\Omega + 2 \rho C_\infty^2 \sum_{\alpha=1}^{N(h)} \int_{\Omega \cap \omega_\alpha^h} \left| \nabla (u - u_\alpha^{hp}) \right|^2 d\Omega \\
\leq\ & 2 \frac{C_G^2}{h_\alpha^2} \rho \sum_{\alpha=1}^{N(h)} C_1^2(\alpha, h, p) \left\| u \right\|_{H^l(\Omega \cap \omega_\alpha^h)}^2 + 2 \rho C_\infty^2 \sum_{\alpha=1}^{N(h)} C_2^2(\alpha, h, p) \left\| u \right\|_{H^l(\Omega \cap \omega_\alpha^h)}^2 \\
\leq\ & 2 \frac{C_G^2}{h_\alpha^2} \rho \max_{\alpha=1,\dots,N(h)} C_1^2(\alpha, h, p) \rho \left\| u \right\|_{H^l(\Omega)}^2 + 2 \rho C_\infty^2 \max_{\alpha=1,\dots,N(h)} C_2^2(\alpha, h, p) \rho \left\| u \right\|_{H^l(\Omega)}^2
\end{aligned}
$$

∎

Suppose now that in Sections 3.2 and 3.3 we had defined $\boldsymbol{\Xi}_\alpha^{hp} := \boldsymbol{X}_\alpha^{hp}$ then we could carry over all the proofs given there since as in the case of the space $\boldsymbol{\Xi}_\alpha^{hp}$, $\mathcal{P}_p \subset \boldsymbol{X}_\alpha^{hp}$. We would then conclude that

**Theorem 3.14** *Suppose that the following holds for some integers $m \geq 0$, $p \geq 0$ and for some numbers $r, s \in [1, \infty]$*

$$W^{p+1,r}(\widehat{\Omega \cap \omega_\alpha^h}) \hookrightarrow W^{m,s}(\widehat{\Omega \cap \omega_\alpha^h})$$

$$\mathcal{P}_p(\widehat{\Omega \cap \omega_\alpha^h}) \subset \widehat{\boldsymbol{X}}_\alpha^{hp} \subset W^{m,s}(\widehat{\Omega \cap \omega_\alpha^h})$$

*Let $(\widehat{\Omega \cap \omega_\alpha^h}, \widehat{\boldsymbol{X}}_\alpha^{hp}, \widehat{\mathbb{L}}_\alpha^2)$ be a ball with $\widehat{\boldsymbol{X}}_\alpha^{hp}$ and $\widehat{\mathbb{L}}_\alpha^2$ defined as before. Then there exists a constant $C(\widehat{\Omega \cap \omega_\alpha^h}, \widehat{\boldsymbol{X}}_\alpha^{hp}, \widehat{\mathbb{L}}_\alpha^2)$ such that, for any h-affine equivalent ball $(\Omega \cap \omega_\alpha^h, \boldsymbol{X}_\alpha^{hp}, \mathbb{L}_\alpha^2)$ and all functions $u \in W^{p+1,r}(\Omega \cap \omega_\alpha^h)$*

$$\boxed{\left| u - \Pi_\alpha^2 u \right|_{m,s,(\Omega \cap \omega_\alpha^h)} \leq C(\widehat{\Omega \cap \omega_\alpha^h}, \widehat{\boldsymbol{X}}_\alpha^{hp}, \widehat{\mathbb{L}}_\alpha^2) h_\alpha^{p+1-m+\frac{n}{s}-\frac{n}{r}} \left| u \right|_{p+1,r,(\Omega \cap \omega_\alpha^h)}} \tag{3.8}$$

*where $h_\alpha$ is the parameter that appears in the h-affine mapping between $(\widehat{\Omega \cap \omega_\alpha^h})$ and $(\Omega \cap \omega_\alpha^h)$.*

**Theorem 3.15** *Suppose that the conditions of Theorem 3.14 hold for all master balls $(\widehat{\Omega \cap \omega_\alpha^h}, \widehat{\boldsymbol{X}}_\alpha^{hp}, \widehat{\mathbb{L}}_\alpha^2)$. Let $u \in H^{p+1}(\Omega)$, $p \geq 0$, then for fixed $h$ and $p$ there is $u_{hp} \in \boldsymbol{X}^{hp}$ such that*

$$
\begin{aligned}
\|u - u_{hp}\|_{L^2(\Omega)} &\leq \rho C_\infty \max_{\alpha=1,\ldots,N(h)} C_\alpha h^{p+1} \|u\|_{H^{p+1}(\Omega)}, \\
|u - u_{hp}|_{H^1(\Omega)} &\leq \sqrt{2}\rho \max_{\alpha=1,\ldots,N(h)} (C_G C_\alpha + C_\infty C_\alpha) h^p \|u\|_{H^{p+1}(\Omega)}
\end{aligned}
$$

*where the constants $C_\infty$ and $C_G$ where defined in Assumption 3.10, the constant $C_\alpha = C(\widehat{\Omega \cap \omega_\alpha^h}, \widehat{\boldsymbol{X}}_\alpha^{hp}, \widehat{\mathbb{L}}_\alpha^2)$ is the same as in Theorem 3.14 and $h = \max_{\alpha=1,\ldots,N(h)} h_\alpha$.*

**Proof:** The above relations are direct consequences of Theorems 3.13 and 3.14 ∎

# 4 Numerical Experiments

In this section we perform some numerical experiments to investigate the approximating properties of the *hp* cloud functions introduced in previous sections. The $h$ and $p$ convergence of the method are investigated and the results compared with the *a-priori* error estimate derived in the previous section.

In the $h$ version of the method the parameters $k$ and $p$ are kept fixed and the size $h_\alpha$ of the balls $\omega_\alpha$ are changed. Of course this has to be followed by an increase in the number of nodes in the discretization when the sizes of the balls are decreased.

The $p$ version of the method can have more than one variant. One, for example, can fix the size $h_\alpha$ of the balls and change the parameter $p$ keeping $k$ fixed. Another possibility would be to increase simultaneously $k$ and $p$. Nonetheless, our analysis in Section 3 has shown that the constant that appears in the error estimate given by Theorem 3.8 do not depend on $k$, but only on $p$. Thus, may not be advantageous to increase the value of $k$.

In all the numerical experiments we used a cubic b-spline weight function that is a slightly modified version of a kernel function widely used in the SPH

Method [45].

$$\mathcal{W}_\alpha(\boldsymbol{y}) := W_\alpha(z) := W(z_\alpha) \tag{4.1}$$

where

$$z_\alpha := \frac{2\|\boldsymbol{y} - \boldsymbol{x}_\alpha\|_{\mathbb{R}^n}}{h_\alpha} \equiv \frac{2\,\|\boldsymbol{r}_\alpha\|_{\mathbb{R}^n}}{h_\alpha} \equiv \frac{2u_\alpha}{h_\alpha}$$

and

$$W(z_\alpha) := \begin{cases} \frac{C}{h_\alpha^n}\left[1 - \frac{3}{2}z_\alpha^2 + \frac{3}{4}z_\alpha^3\right] & \text{if } 0 \le z_\alpha < 1 \\ \frac{C}{4h_\alpha^n}\left[2 - z_\alpha\right]^3 & \text{if } 1 \le z_\alpha < 2 \\ 0 & \text{if } z_\alpha \ge 2 \end{cases} \tag{4.2}$$

where $n$ is the dimension of the problem and $C$ is a constant given by

$$C = \begin{cases} \frac{2}{3} & \text{if } n = 1 \\ \frac{10}{7\pi} & \text{if } n = 2 \\ \frac{1}{\pi} & \text{if } n = 3 \end{cases}$$

The derivatives of the weight function are given by

$$\frac{\partial \mathcal{W}_\alpha}{\partial y_i} = \frac{dW}{dz_\alpha}\frac{\partial z_\alpha}{\partial y_i} = \frac{dW}{dz_\alpha}\frac{dz_\alpha}{u_\alpha}\frac{\partial u_\alpha}{\partial y_i} = \frac{dW}{dz_\alpha}\frac{2}{h_\alpha}\frac{r_i}{u_\alpha} \tag{4.3}$$

where

$$\frac{dW}{dz_\alpha} = \begin{cases} \frac{3C}{h_\alpha^n}\left[-z_\alpha + \frac{3}{4}z_\alpha^2\right] & \text{if } 0 \le z_\alpha < 1 \\ \frac{-3C}{4h_\alpha^n}\left[2 - z_\alpha\right]^2 & \text{if } 1 \le z_\alpha < 2 \\ 0 & \text{if } z_\alpha \ge 2 \end{cases} \tag{4.4}$$

## 4.1 $L^2$ Projection of a Smooth Function in 1-D

We computed the $L^2$ projection, $U_{hp}$, of the function $U = \sin(4\pi x),\ x \in [0,1]$, on a subspace spanned by cloud functions. The function $U$ is shown in Figure 4.1. Many subfamilies of the general family $\mathcal{F}_N^{k,p}$ were tested. The results for the $h$ and $p$ convergence of these subfamilies are presented and analyzed next.

### 4.1.1 $h$ Convergence

The behavior of the error $U - U_{hp}$ in the $L^2$ norm when uniform $h$ refinement was performed is investigated in this section. The number of nodes ranged from 9 to 129, always evenly distributed in the interval $[0,1]$ with one node at each end of the domain. The nine node distribution is shown in Figure 4.2. In the experiments $k$ and $p$ ranged from 0 to 2.

Figure 4.3 shows the $h$ convergence in the $L^2$ norm of $U_{hp}$. The results are shown for three sets of functions; the sets $\mathcal{F}_N^{k=p=0}$, $\mathcal{F}_N^{k=p=1}$ and $\mathcal{F}_N^{k=p=2}$. The curves show that the rate of convergence is equal to $p+1$ which is in agreement with the estimate given by Theorem 3.15.

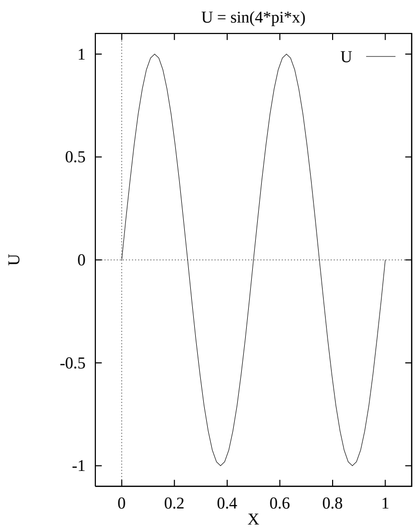


Figure 4.1: Smooth Function for Test 1.

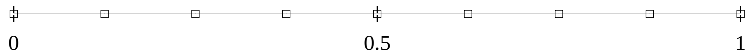


Figure 4.2: Nine Nodes Arrangement for Test 1.

Figure 4.4 shows the results when the basis functions from the sets $\mathcal{F}_N^{k=0,p=0}$, $\mathcal{F}_N^{k=0,p=1}$ and $\mathcal{F}_N^{k=0,p=2}$ were used. That is, we compared the rates of convergence when using different values of $p$ and $k$ were kept constant. The curves show that the rate of convergence is equal to $p+1$, again in agreement with Theorem 3.15. Another test on the dependence of the rate of convergence on $k$ and $p$ was performed by comparing the rates of convergence when using different values of $k$ while keeping $p$ constant. The results are shown on Figure 4.5. It can be observed that the rate of convergence is always approximately equal to $p+1$ and does *not* depend on the value of $k$. Figure 4.6 shows the same results, but this time the error $U - U_{hp}$ was plotted against the number of degrees of freedom instead of the size of the balls. The conclusions in this case are the same as before.

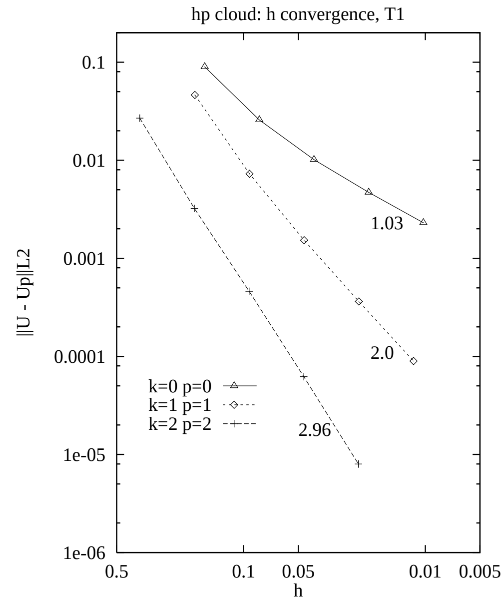


Figure 4.3: $h$ Convergence $L^2$ Norm, $0 \leq k,\ p \leq 2$.

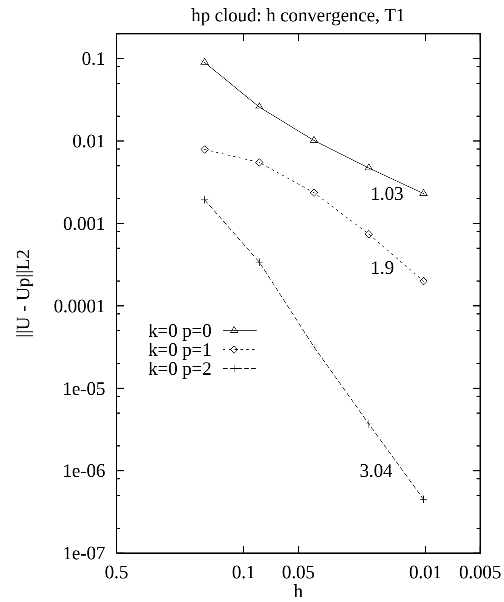


Figure 4.4: $h$ Convergence $L^2$ Norm, $k = 0\ \ 0 \leq p \leq 2$

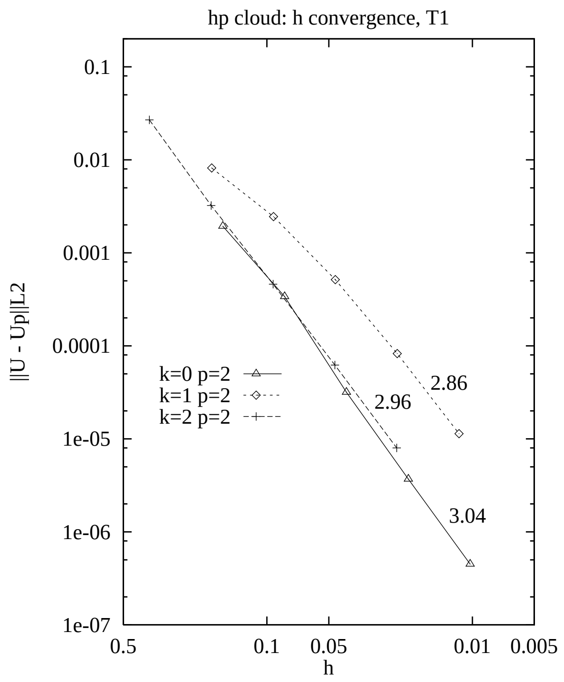


Figure 4.5: $h$ Convergence $L^2$ Norm, $p = 2 \;\; 0 \leq k \leq 2$.

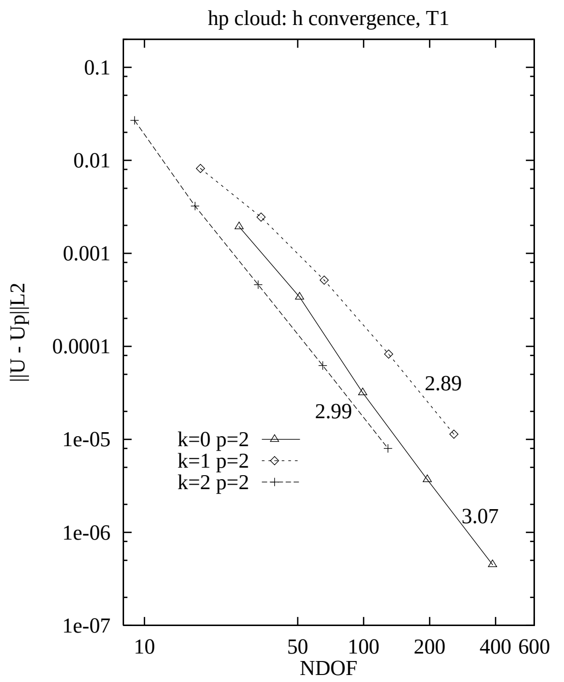


Figure 4.6: $h$ Convergence $L^2$ Norm, $p = 2 \;\; 0 \leq k \leq 2$.

### 4.1.2 $p$ Convergence

In this section we analyze the effect of uniform $p$ enrichment of the $hp$ cloud space on the error $U - U_{hp}$ measured in the $L^2$ and $H^1$ norms. More than one variant of the $p$ version are investigated. We will denote by variant $\wp_1$ the case when $k$ and $p$ are simultaneously increased and by variant $\wp_2$ the case when $k$ is kept at a fixed value and $p$ is increased. In all experiments reported in this section the nine node arrangement shown in Figure 4.2 was used and the algorithm described in Section 2.4.1 was used to automatically set the size of the balls.

Figure 4.7 shows the results for the variant $\wp_1$ with $1 \leq k = p \leq 5$ and for the variant $\wp_2$ when $k = 0,\ 1 \leq p \leq 7$; $k = 1,\ 1 \leq p \leq 7$ and $k = 2,\ 2 \leq p \leq 7$. The variant $\wp_2$ with $k = 0$ gave, for all values of $p$, the smallest error. The rate of convergence *increased with* $p$ in all experiments using the variant $\wp_2$. As Figure 4.7 shows, the rate ranged from 2.02 to 17.26 when the variant $\wp_2$ with $k = 0$ was used. This behavior is typical of spectral methods like the $p$ version of the finite element method. These results confirm the dependence on $p$ of the constant that appears in the error estimate of Theorem 3.15. The results obtained with variant $\wp_1$ are also shown in Figure 4.7. It can be observed that this variant did *not* converge. This is a consequence that the constant of the error estimate (3.7) does not depend on $k$.

Figure 4.7 shows that for a fixed value of $p$ the variant $\wp_2$ with $k = 0$ gave the smallest error. Nonetheless one can not conclude that the choice of $k = 0$ is the best in terms of error versus number of degrees of freedom. That is because the definition of the family $\mathcal{F}_N^{k,p}$ given in (2.7) implies that $dim\{\mathcal{F}_N^{k=0,p}\} > dim\{\mathcal{F}_N^{k=1,p}\} > dim\{\mathcal{F}_N^{k=2,p}\}$. Figure 4.8 shows the same results of Figure 4.7, but this time we plotted the error in the $L^2$ projection versus the number of degree of freedom. It can be observed that in all the cases ($k = 0,\ k = 1$ or $k = 2$) the error, for a fixed number of degrees of freedom, is almost the same, with only a slight advantage in favor of the case $k = 0$. We should now recall that the definition of the moving least squares functions $\varphi_\alpha$ given by (2.3) involves the inversion of a matrix of dimensions $(dim\mathcal{P}) \times (dim\mathcal{P})$ and that $dim\mathcal{P}$ is at least equal to $\binom{k+n}{n}$. Thus we conclude that the family $\mathcal{F}_N^{k=0,p}$ is the most economical since it does not involve the inversion of any matrix in the construction of the moving least squares functions $\varphi_\alpha$ and gives the same level of accuracy of the other families for a fixed number of degree of freedom. Figures 4.9 and 4.10 are the equivalents of Figures 4.7 and 4.8, respectively, when measuring the error $U - U_{hp}$ in the $H^1$ norm. The conclusions are the same as before.

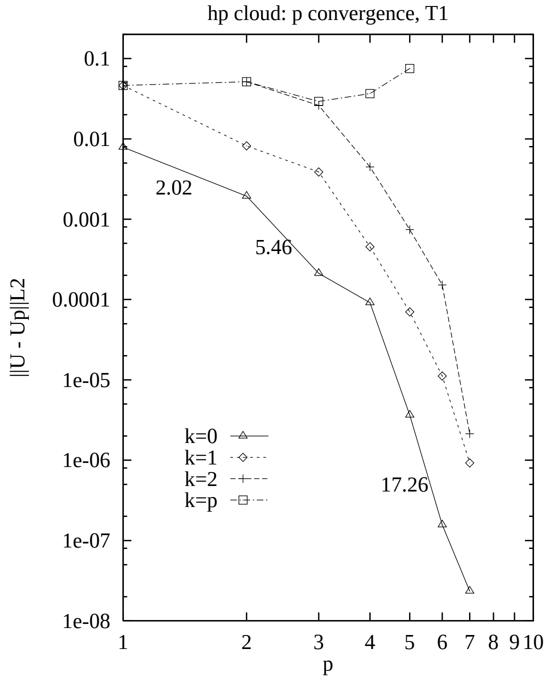


Figure 4.7: $p$ Convergence $L^2$ Norm, $0 \leq k \leq 2,\ 1 \leq p \leq 7$.

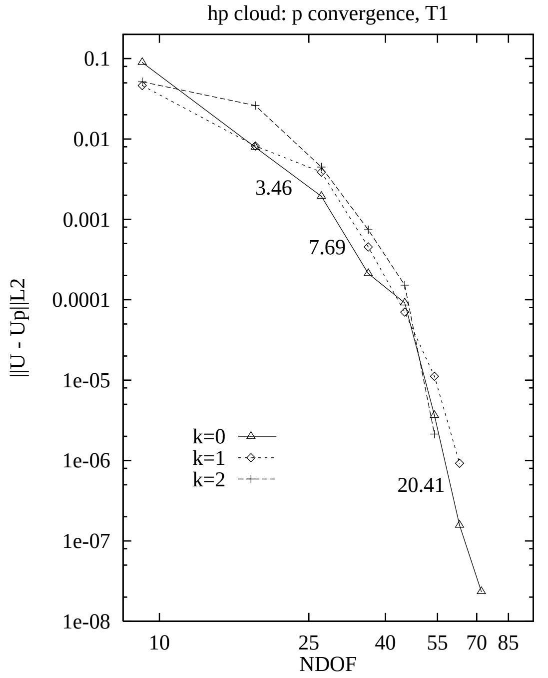


Figure 4.8: $p$ Convergence $L^2$ Norm, $0 \leq k \leq 2,\ 0 \leq p \leq 7$.

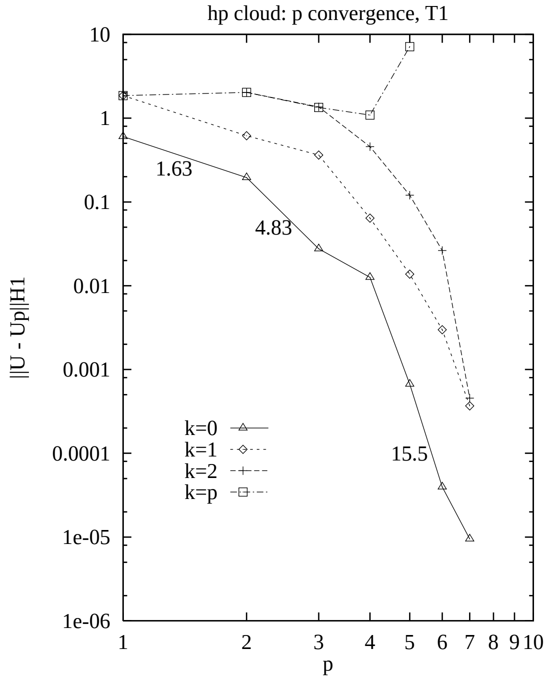


Figure 4.9: $p$ Convergence $H^1$ Norm, $0 \leq k \leq 2,\ 1 \leq p \leq 7$.

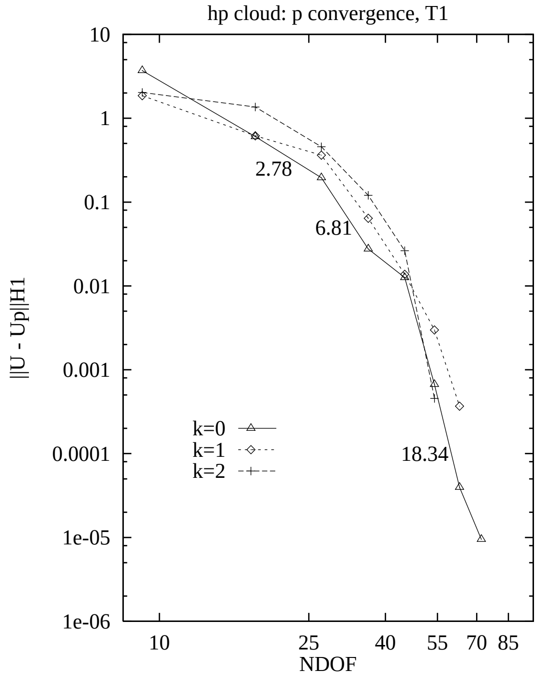


Figure 4.10: $p$ Convergence $H^1$ Norm, $0 \leq k \leq 2,\ 0 \leq p \leq 7$.

## 4.2 $L^2$ Projection of a Rough function

We shall now illustrate the performance of the cloud functions to approximate a function with a high gradient in some small part of the domain. The model function is

$$U = (1-x)[\tan^{-1}(\alpha(x-x_0)) + \tan^{-1}(\alpha x_0)] \qquad \Omega = [0,1]$$

We tested the case when $\alpha = 50$ ($\alpha$ controls the magnitude of the gradient at $x_0$) with $x_0 = 0.2$. $U$ and $dU/dx$ are shown in Figures 4.12 and 4.13, respectively.

We performed a $p$ convergence analysis using the variant $\wp_2$ and the same families as in the previous experiment. The nine node arrangement shown in Figure 4.2 was also used in this experiment. Figure 4.14 shows the results when $k = 0$, $1 \leq p \leq 7$; $k = 1$, $1 \leq p \leq 7$ and $k = 2$, $2 \leq p \leq 7$. Figure 4.15 shows the same results of Figure 4.14 with the exception that the abscissa shows the number of degrees of freedom instead of the value of $p$. We can draw the same conclusions as in the previous test case, namely: We got spectral convergence with the rate of convergence ranging from 0.90 to 8.30 and the family $\mathcal{F}_N^{k=0,p}$ was the best choice.

We next investigated the possibility of getting even higher rates of convergence using a node distribution that takes into account the behavior of the function $U$ around $x_0 = 0.2$. We used the graded node arrangement shown in Figure 4.11. The results obtained are plotted against the previous ones in Figure 4.16. We can observe a clear increase in the rate of convergence when the graded node distribution was used. The results shown are for the family $\mathcal{F}_N^{k=0,p}$.

The conclusion from this experiment is that like in the finite element method, the use of adaptivity to automatically select the node arrangement and spectral orders in the $hp$ cloud method can possibly lead to substantial savings in computations.

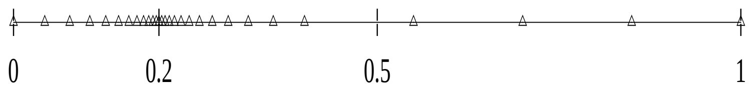


Figure 4.11: Graded Node Arrangement for Test 2.

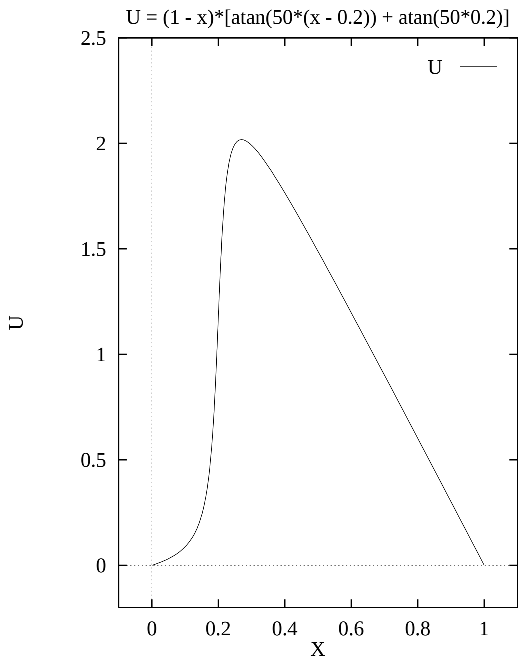


Figure 4.12: Rough Function for Test 2.

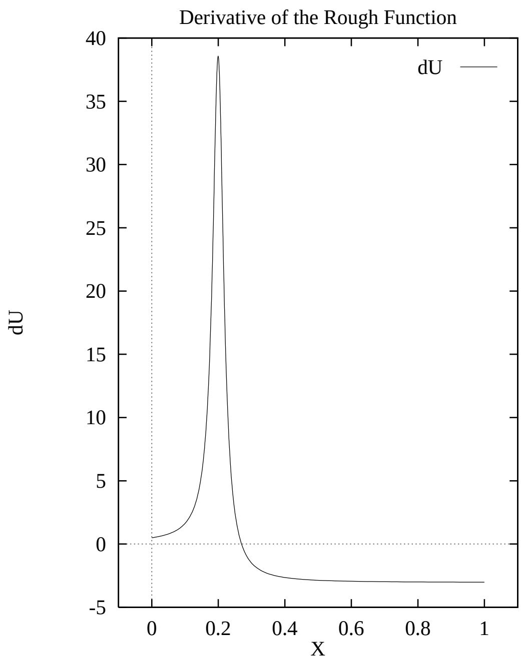


Figure 4.13: Derivative of the Rough Function.

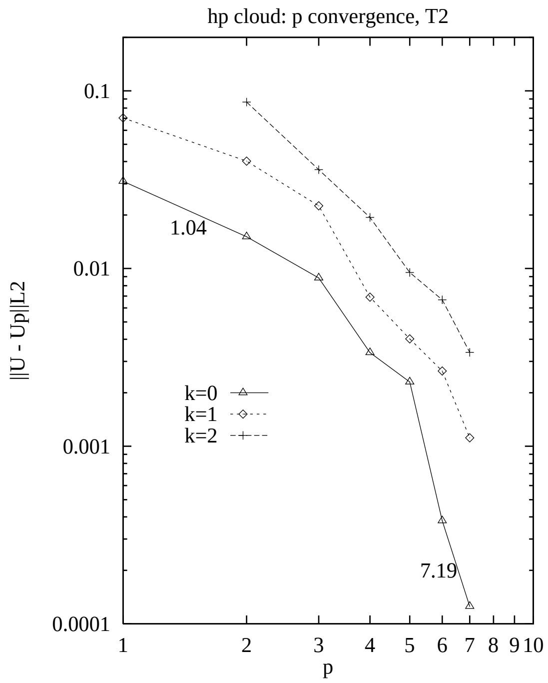


Figure 4.14: $p$ Convergence $L^2$ Norm, $0 \leq k \leq 2,\ 1 \leq p \leq 7$.

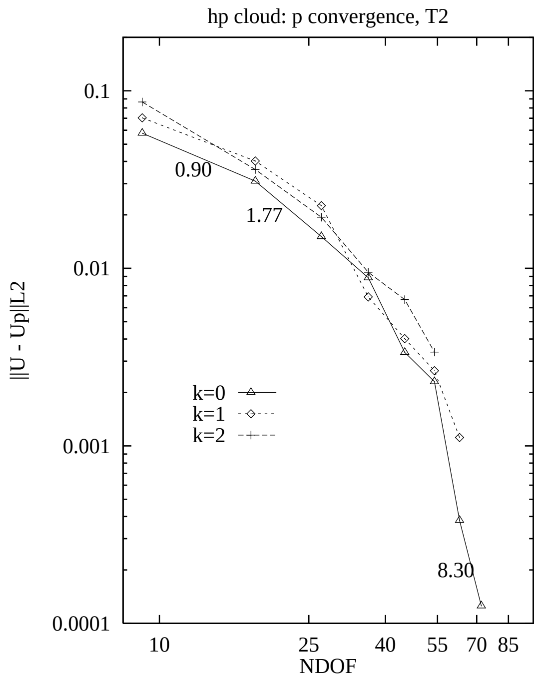


Figure 4.15: $p$ Convergence $L^2$ Norm, $0 \leq k \leq 2,\ 1 \leq p \leq 7$.

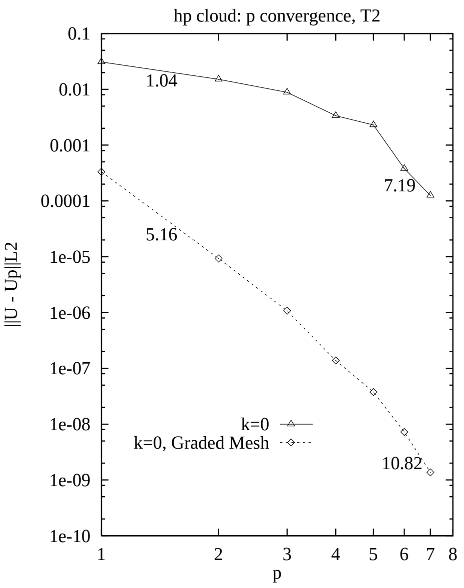


Figure 4.16: $p$ Convergence for Graded and Uniform Node Arrangement.

## 4.3 $L^2$ Projection in 2-D

We shall now investigate the effect of using nonuniform node arrangements and nonuniform ball sizes, $h_\alpha$, in two dimensions. We computed the $L^2$ projection of the function

$$U = \frac{5}{2}x^3 - \frac{3}{2}x + \frac{5}{2}y^3 - \frac{3}{2}y \qquad \Omega = [-1,1] \times [-1,1]$$

on the space spanned by $\mathcal{F}_N^{k=1,p=3}$.

We used the uniform node arrangement shown in Figure 2.9 and the nonuniform node arrangement shown in Figure 4.17. In both cases the algorithm described in Section 2.4.1 was used to automatically set the radius, $h_\alpha$, of the balls. From Theorem 2.7 we have that $U \in span\{\mathcal{F}_N^{k=1,p=3}\}$ and thus we must have an error of the order of the round off errors. Both nodes arrangements gave the following results

- $max|U - U_{hp}| = O(10^{-10})$
- $max|\frac{\partial U}{\partial x} - \frac{\partial U_{hp}}{\partial x}| = max|\frac{\partial U}{\partial y} - \frac{\partial U_{hp}}{\partial y}| = O(10^{-9})$

in agreement with Theorem 2.7. Figure 4.18 shows the projection of $U$ in the span of $\{\mathcal{F}_N^{k=1,p=3}\}$ and Figure 4.19 shows its derivative with respect to $x$.

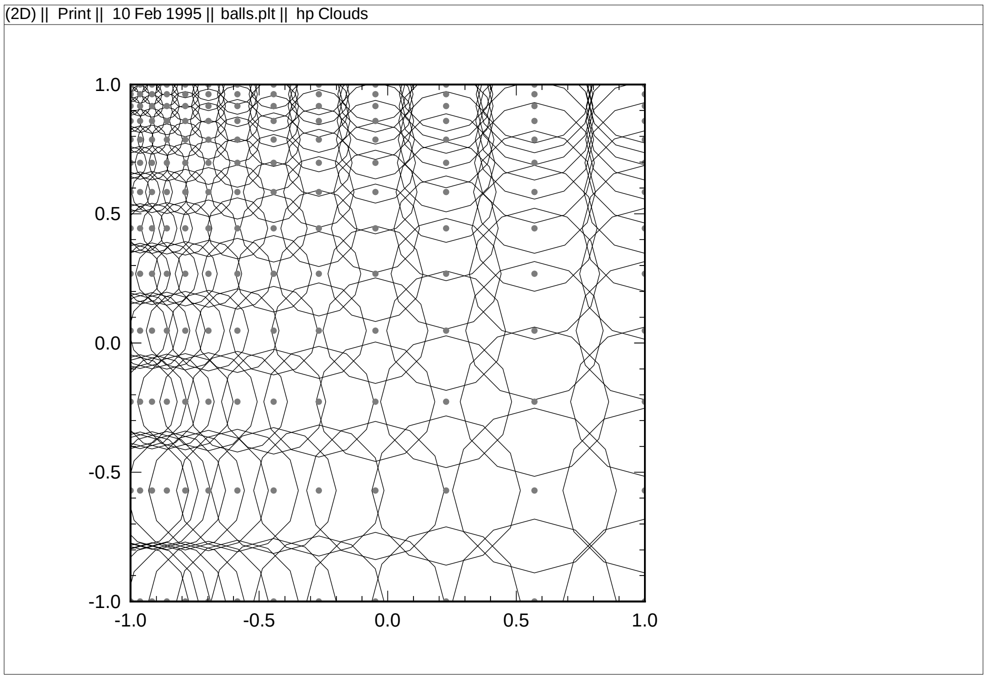


Figure 4.17: Nonuniform Node Arrangement and Support of Functions.

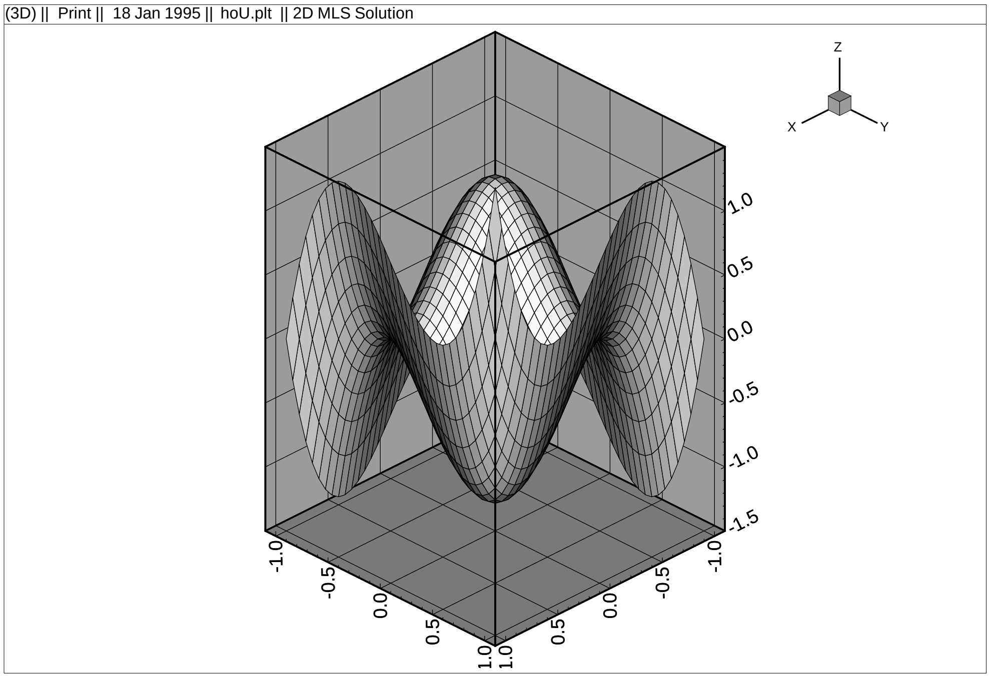


Figure 4.18: Projection of $U$ on $span(\mathcal{F}_N^{k=1,p=3})$. $max|U - U_{hp}| = O(10^{-10})$.

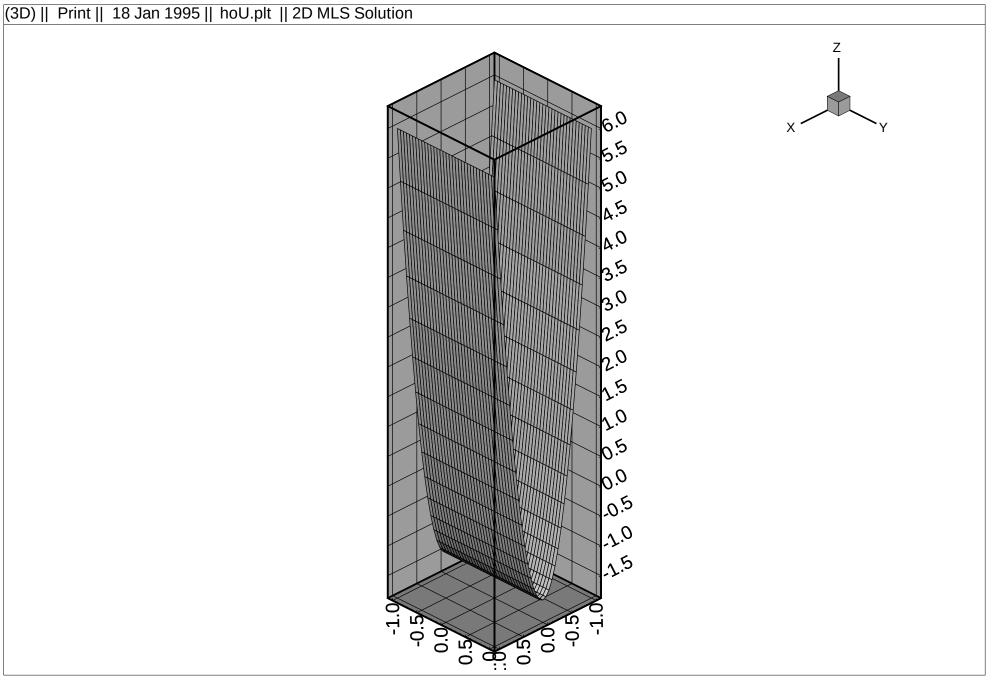


Figure 4.19: $\frac{\partial U_{hp}}{\partial x}$ of the Projection of $U$ on $span(\mathcal{F}_N^{k=1,p=3})$. $max|\frac{\partial U}{\partial x} - \frac{\partial U_{hp}}{\partial x}| = O(10^{-9})$.

# 5 Solution of BVPs Using the Families $\mathcal{F}_N^{k,p}$ and the Galerkin Method—The *hp* Cloud Method

## 5.1 Introduction

In the following sections the *hp* cloud method denotes a numerical technique to solve boundary value problems where one uses the *hp* cloud functions to construct appropriate finite dimensional subspaces of functions used in the Galerkin method. The use of the Galerkin method is only a question of choice. Other techniques, such as collocation, can be used as well.

In this section one and two dimensional boundary-value problems are solved using the *hp* cloud method. Some of the results are compared with the solutions obtained using the FEM.

## 5.2 Heat Conduction Equation in One Dimension

The following boundary-value problem was solved using the $p$ version of the $hp$ cloud method:

Find $u = u(x)$ such that

$$\begin{aligned} -\frac{d^2u}{dx^2} &= f \qquad in\ \Omega = [-1, 1] \\ u &= u_1 \qquad at\ x = -1 \\ \frac{du}{dx} &= \sigma_2 \qquad at\ x = 1 \end{aligned}$$

The parameters $f, u_1$ and $\sigma_2$ where chosen such that the solution $u$ is given by

$$u = \frac{35}{8}x^4 - \frac{15}{4}x^2 + \frac{3}{8}$$

that is, the Legendre polynomial of fourth degree.

A five node arrangement uniformly distributed in the domain was used in the computations. The value of the parameter $k$ was kept fixed at zero and the parameter $p$ ranged form 0 to 3. The discretization using the family $\mathcal{F}_N^{k=0,p=4}$, gave, as expected, the exact solution within round off and quadrature errors.

This problem was also solved using the $p$ version of the finite element method. A uniform mesh of four elements was used in the discretization. The degree of the finite elements ranged form 1 to 3.

The first difficulty in comparing the $hp$ cloud method with the FEM is to decide how to perform a fair comparison. One can compare based on the value of $p$ or on the number of degrees of freedom. We opted to compare the solutions corresponding to approximately the same number of degrees of freedom.

Figure 5.1 shows the pointwise error, $u' - u_p'$, when using the $hp$ cloud method with $k = 0,\ p = 0$ and the FEM with $p = 1$. In both cases the number of degrees of freedom is equal to 5. It can be observed that the maximum norm of the error is almost the same in both cases but the derivative of the $hp$ cloud solution does not exhibit discontinuities like the derivative of the FE solution. The results when $k = 0,\ p = 1$ in the $hp$ cloud method and $p = 2$ in the FEM are shown in Figure 5.2. The error in the maximum norm of the $hp$ cloud flux is about three times smaller than the corresponding error of the FE flux. It can be observed that the $hp$ cloud solution is at least a $C^1(\Omega)$ function. Figure

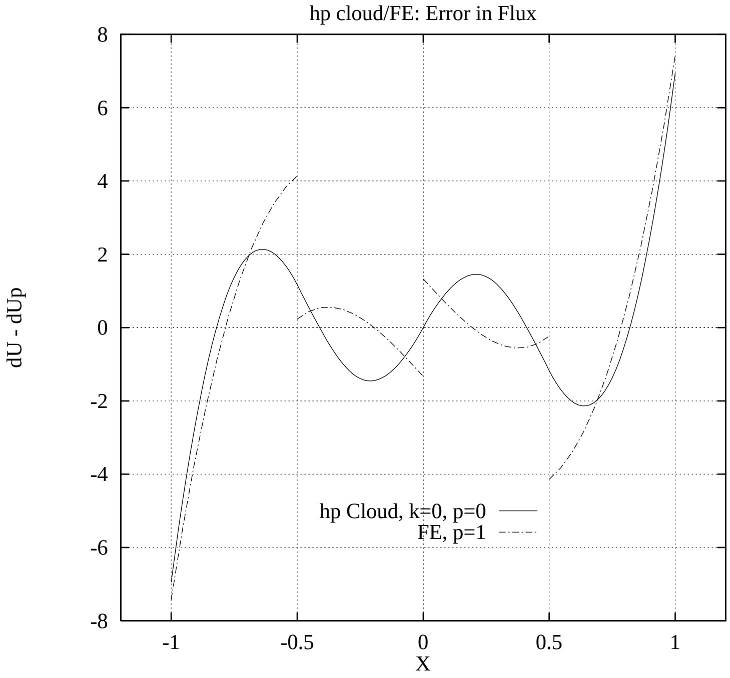


Figure 5.1: *hp* Cloud and FE error in Flux

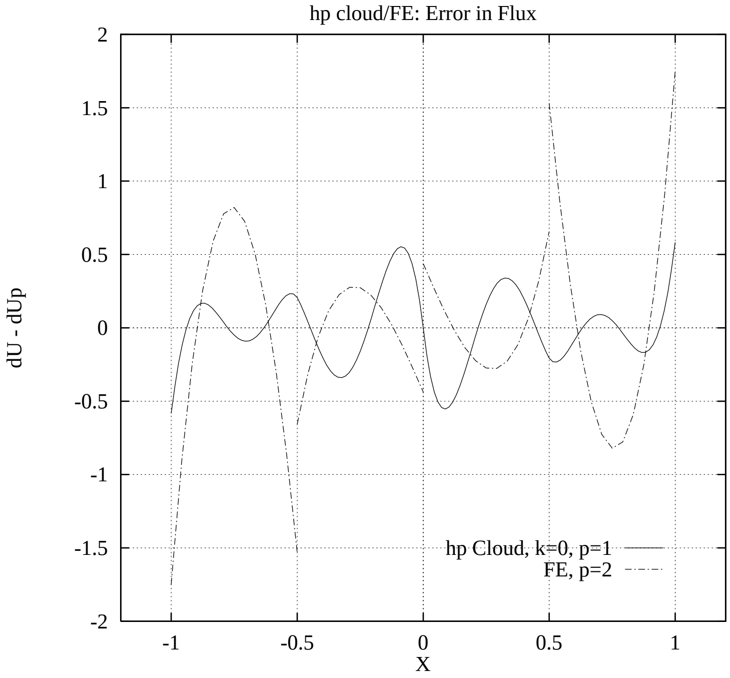


Figure 5.2: *hp* Cloud and FE error in Flux

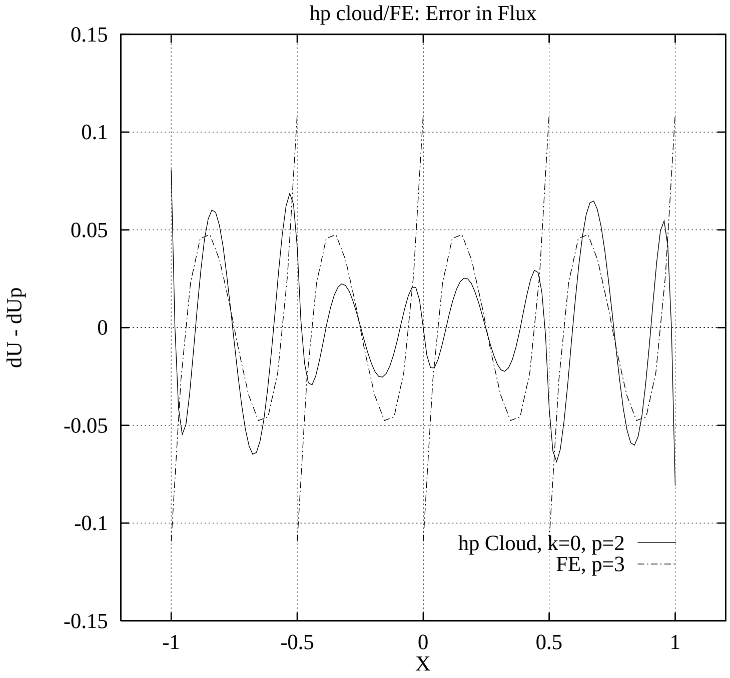


Figure 5.3: *hp* Cloud and FE error in Flux

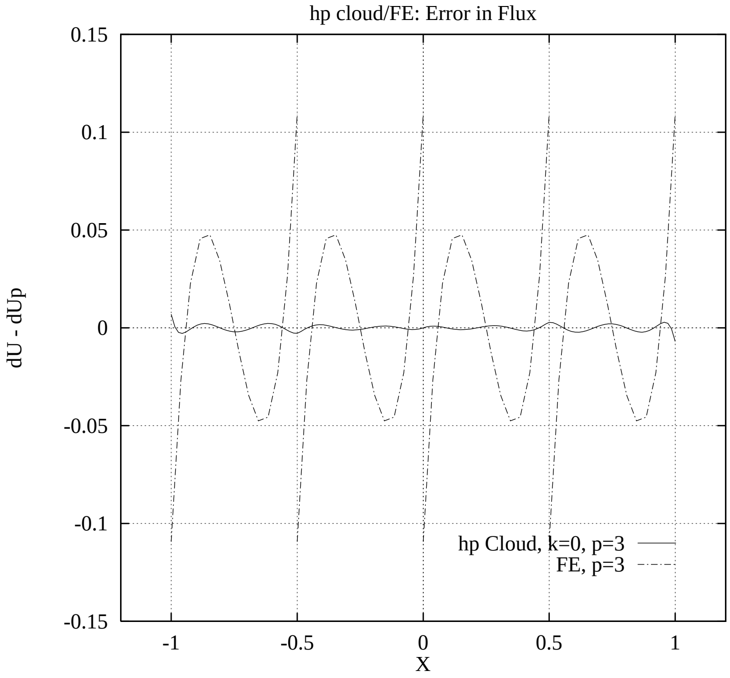


Figure 5.4: *hp* Cloud and FE error in Flux

5.3 corresponds to the case of the $hp$ cloud method with $k = 0,\ p = 2$ and the FEM with $p = 3$. The conclusions are the same as before. Finally, in Figure 5.4 we compared the error in the $hp$ cloud flux when $k = 0,\ p = 3$ with the error in the FE flux when $p = 3$. The $hp$ cloud approximation of the flux is remarkably better then the FE approximation. However, note that the $hp$ cloud solution was obtained using more degrees of freedom than used in the FEM.

## 5.3 Poisson's Equation on a Square Domain.

In this section we focus on the solution of a Poisson problem in which a function $u = u(\boldsymbol{x})$ is sought satisfying

$$
\begin{aligned}
-\Delta u &= f \qquad in\ \Omega = [-1,1] \times [-1,1] \\
-\frac{\partial u}{\partial n} &= \hat{g}(x,y) \qquad on\ \Gamma_N \\
-\frac{\partial u}{\partial n} &= (u - u_\infty) \qquad on\ \Gamma_C \\
u &= 0 \qquad on\ \Gamma_D
\end{aligned}
$$

where $\Delta$ is the Laplacian, and $f$, $\hat{g}(x,y)$ and $u_\infty$ were chosen such that the solution $u$ is

$$u = (1 - x^{11}) \cosh(\pi y)$$

The domain $\Omega$ and the node arrangement used are represented in Figure 5.5.

The above problem was solved using its weak formulation and the Galerkin method. The subspaces for the Galerkin method were built using the $hp$ cloud functions described in previous sections. The Dirichlet boundary condition was imposed using Lagrange multipliers.

The variant $\wp_2$ of the $p$ version of the cloud method described in Section 4.1.2 was used. The value of $k$ was kept fixed at $k = 0$ and $p$ ranged form 0 to 7. Figure 5.6 shows the error $U - U_p$, measured in the $H^1$ and $L^2$ norms, versus the value of $p$. The rate of convergence in the $L^2$ norm ranged from 1.58 to 9.14 and in the $H^1$ norm it ranged from 1.03 to 9.67. This kind of behavior is typical of spectral methods. Figure 5.7 shows the error $U - U_p$ versus the total number of degrees of freedom.

Figure 5.8 shows the cloud solution $U_p$ and Figure 5.9 shows its $x$ derivative. It can be observed that $\partial U_p/\partial x$ is continuous and it is therefore unnecessary to perform any flux smoothing.

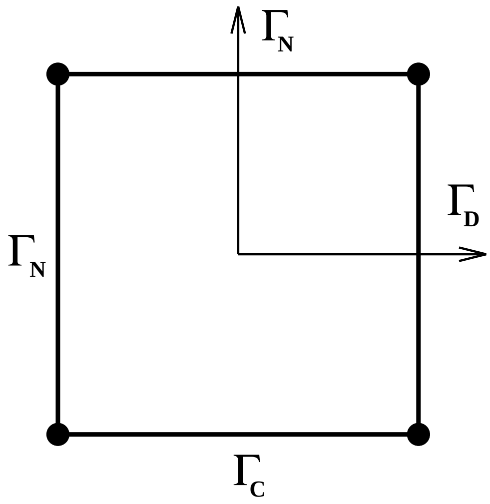


Figure 5.5: Domain and node arrangement for 2-D BVP.

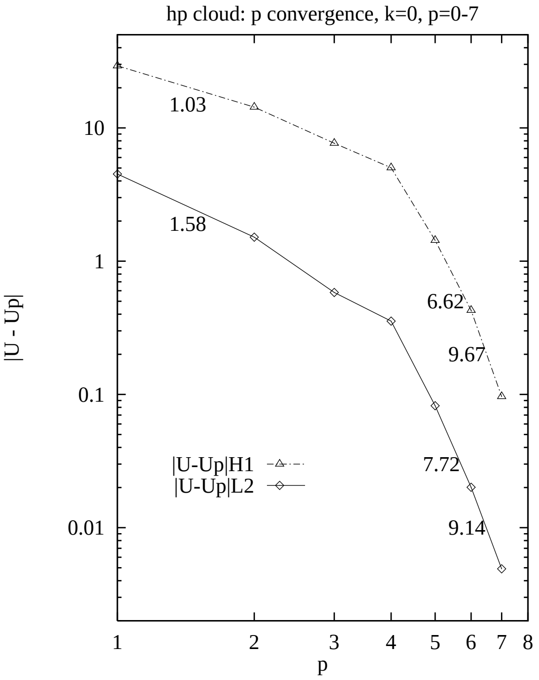


Figure 5.6: $p$ Convergence, $k = 0$, $0 \leq p \leq 7$

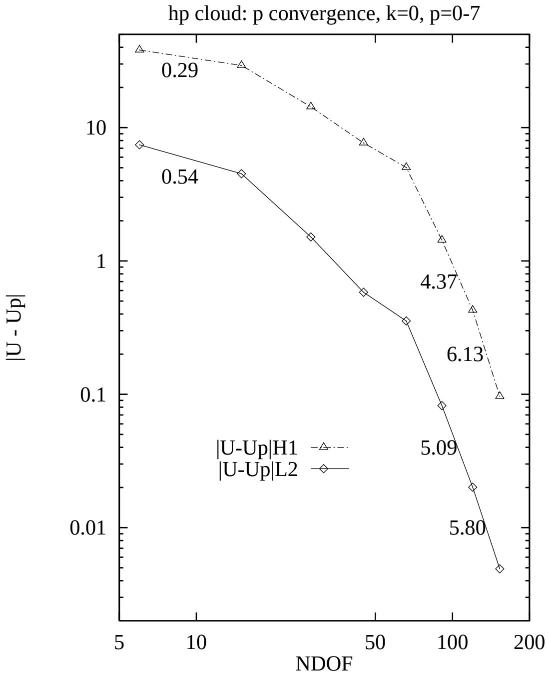


Figure 5.7: $p$ Convergence, $k = 0$, $0 \leq p \leq 7$

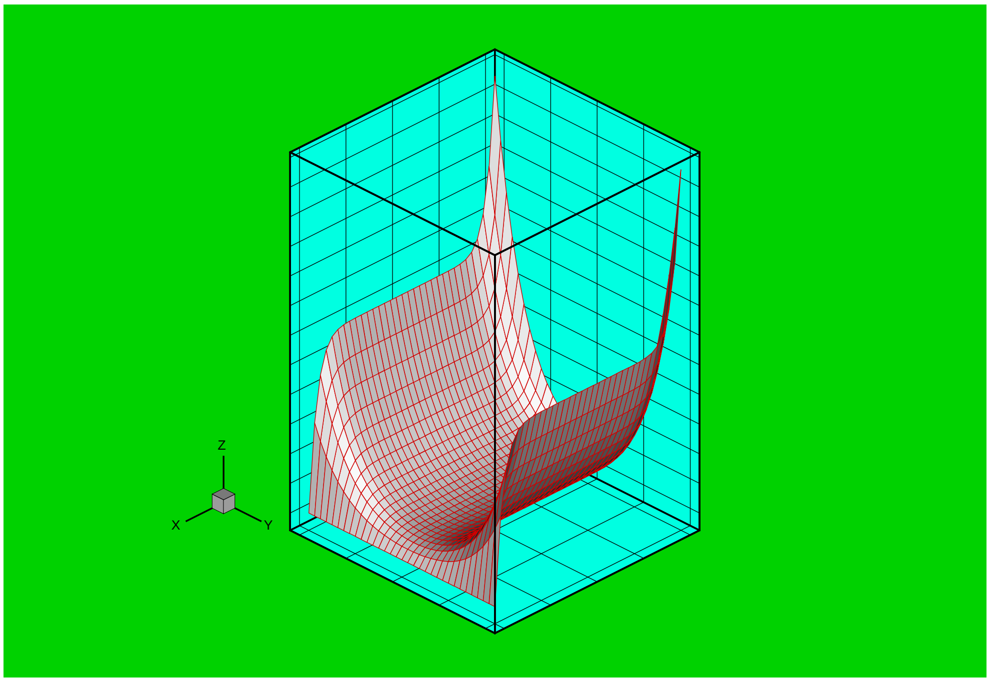


Figure 5.8: $hp$ cloud solution.

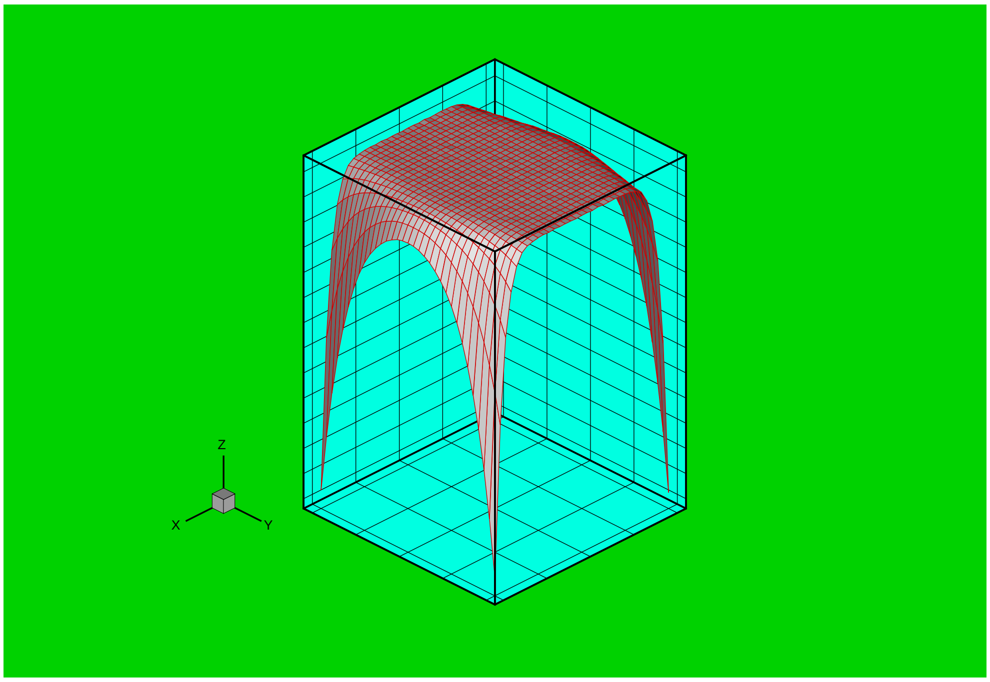


Figure 5.9: $x$ derivative of the $hp$ cloud solution.

# 6 Conclusions

In this paper a meshless method to solve a large class of boundary-value problem is proposed. The method involves the placement of $hp$ approximations in spheres centered at arbitrary points in the domain. The method can be used in one, two as well in three dimensions. *a-priori* error estimates for the $h$ version of the method have been derived. The method showed to be robust enough to handle problems where the solution exhibits localized behavior, such as boundary layers. The numerical experiments showed that one can expect exponential rates of convergence when the $hp$ version of the method is used. Another remarkable feature of the $hp$ cloud method is the regularity of the solution one can get. We where able to obtain $C^2(\Omega)$ approximate solutions of a second order boundary-value problem without any difficult. Higher order of regularity can be attained at no extra cost.

Much additional work remains to be done but the results presented in this paper show that the $hp$ cloud method has a great potential to become a very competitive method for the solution of a broad class of boundary-value problems.

**Acknowledgment:** *The support of this work by the Army Research Office under contract DAAL03-92-G-0253 and the CNPq Graduate Fellowship Program's support of Armando Duarte is gratefully acknowledged.*

# References

[1] R. Adams. *Sobolev Spaces*. Academic Press, INC., Boston, 1978.

[2] Mark Ainsworth. Personal communication. 1994.

[3] K. Amarantuga, J. R. Williams, S. Qian, and J. Weis. Wavelet-galerkin solutions for one-dimensional partial differential equations. *International Journal for Numerical Methods in Engineering*, 37:2703–2716, 1994.

[4] I. Babuska and W. C. Rheinboldt. Error estimates for adaptive finite element computations. *SIAM J. Numerical Analysis*, 15(4):736–753, 1978.

[5] T. Belytschko, Y. Y. Lu, and L. Gu. Crack propagation by element free galerkin methods. In *Advanced Computational Methods for Material Modeling*, pages 191–205, 1993. AMD-Vol. 180/PVP-Vol. 268, ASME 1993.

[6] T. Belytschko, Y. Y. Lu, and L. Gu. Element-free galerkin methods. *International Journal for Numerical Methods in Engineering*, 37:229–256, 1994.

[7] Arthur P. Boresi and Paul P. Lynn. *Elasticity in Engeneering mechanics*. Prentice-Hall, New Jersew, 1974.

[8] C. K. Chui. *An Introduction to Wavelets*. Academic Press, Boston, 1992.

[9] C. K. Chui, editor. *Wavelets: A Tutorial in Theory and Applications*. Academic Press, Boston, 1992.

[10] Philippe G. Ciarlet. *The Finite Element Method for Elliptic Problems*. North-Holland, Amsterdam, 1978.

[11] Carl deBoor. *A Practical Guide to Splines*. Springer-Verlag, New York, 1978.

[12] L. Demkowicz, A. Karafiat, and T. Liszka. On some convergence results for FDM with irregular mesh. *Computer Methods in Applied Mechanics and Engineering*, 42:343–355, 1984.

[13] L. Demkowicz, J. T. Oden, W. Rachowicz, and O. Hardy. Toward a universal *h-p* adaptive finite element strategy, part 1. constrained approximation and data structure. *Computer Methods in Applied Mechanics and Engineering*, 77:79–112, 1989.

[14] C. A. M. Duarte. A review of some meshless methods to solve partial differential equations. Technical Report 95-06, TICAM, The University of Texas at Austin, 1995.

[15] C. A. M. Duarte and J. T. Oden. Hp clouds–a meshless method to solve boundary-value problems. Technical Report 95-05, TICAM, The University of Texas at Austin, 1995.

[16] Richard Franke. Scattered data interpolation: Test of some methods. *Mathematics of Computation*, 38(157):181–200, 1982.

[17] R. A. Gingold and J. J. Monaghan. Kernel estimates as a basis for general particle methods in hydrodynamics. *Journal of Computational Physics*, 46:429–453, 1982.

[18] R. Glowinski, M. Lawton, M. Ravachol, and E. Tenenbaum. Wavelet solutions of linear and nonlinear elliptic, parabolic and hyperbolic problems in one space dimension. In $9^{th}$ *Int. Conf. on Numerical Methods in Applied Sciences and Engineering, SIAM*, Philadelphia, USA, 1990.

[19] R. L. Hardy. Theory and applications of the multiquadric–biharmonic method. *Computers and Mathematics with Applications*, 19(8/9):163–208, 1990.

[20] G. R. Johnson, E. H. Peterson, and R.A. Stryrk. Incorporation of an sph option into the epic code for a wide range of high velocity impact computations. In *Colloquium on Advances in Smoothed Particle Hydrodynamics*, 1993.

[21] E. J. Kansa. Multiquadrics–a scattered data approximation scheme with applications to computational fluid-dynamics–i surface approximations and partial derivative estimates. *Computers and Mathematics with Applications*, 19(8/9):127–145, 1990.

[22] E. J. Kansa. Multiquadrics–a scattered data approximation scheme with applications to computational fluid-dynamics–ii solutions to parabolic, hyperbolic and elliptic partial differential equations. *Computers and Mathematics with Applications*, 19(8/9):147–161, 1990.

[23] Andrzej Karafiat. On convergence of solutions for fdm with irregular mesh in neumann problem. *Computer Methods in Applied Mechanics and Engineering*, 72:91–103, 1989.

[24] Andrzej Karafiat. Discrete maximum principle for parabolic boundary-value problems. *Annales Polonici Mathematici*, 53(3):253–265, 1991.

[25] P. Lancaster and K. Salkauskas. Surfaces generated by moving least squares methods. *Mathematics of Computation*, 37(155):141–158, 1981.

[26] P. Lancaster and K. Salkauskas. *Curve and Surface Fitting, an Introduction.* Academic Press, San Diego, 1986.

[27] Tadeusz Liszka. An interpolation method for an irregular net of nodes. *International Journal for Numerical Methods in Engineering*, 20:1599–1612, 1984.

[28] Tadeusz Liszka and J. Orkisz. Finite difference method for arbitrary irregular meshes in nonlinear problems of applied mechanics. In *IV SMiRt*, San Francisco, 1977.

[29] Tadeusz Liszka and J. Orkisz. The finite difference method at arbitrary irregular grids and its application in applied mechanics. *Computers and Structures*, 11:83–95, 1980.

[30] Wing Kam Liu and Yijung Chen. Wavelet and multiple scale reproducing kernel methods. Accepted for publication in the International Journal for Numerical Methods in Fluids.

[31] Wing Kam Liu, Sukky Jun, Shaofan Li, Jonathan Adee, and Ted Belytschko. Reproducing kernel particle methods for structural dynamics. Accepted for publication in the International Journal for Numerical Methods in Engineering.

[32] Y. Y. Lu, T. Belytschko, and L. Gu. A new implementation of the element free galerkin method. *Computer Methods in Applied Mechanics and Engineering*, 113:397–414, 1994.

[33] Y. Y. Lu, Ted Belytschko, and M. Tabbara. Element-free galerkin method for wave propagation and dynamic fracture. Accepted for publication in Computer Methods in Applied Mechanics and Engineering.

[34] L. B. Lucy. A numerical approach to the testing of the fission hypothesis. *Astronomical Journal*, 82:1013–1024, 1977.

[35] J. M. Melenk. Finite element methods with harmonic shape functions for solving laplace's equation. Master's thesis, The University of Maryland, 1992.

[36] J. M. Melenk. *On Generalized Finite Element Methods*. PhD thesis, The University of Maryland, 1995.

[37] J. J. Monaghan. Why particle methods work. *SIAM J. Sci. Stat. Comput.*, 3(4):422–433, 1982.

[38] J. J. Monaghan. An introduction to sph. *Computer Physics Communications*, 48:89–96, 1988.

[39] R. A. Nay and S. Utku. An alternative for the finite element method. In *Variational Methods in Engineering*, volume 1, University of Southampton, September 1972.

[40] B. Nayroles, G. Touzot, and P. Villon. Generalizing the finite element method: Diffuse approximation and diffuse elements. *Computational Mechanics*, 10:307–318, 1992.

[41] J. T. Oden and G. F. Carey. *Texas Finite Element Series Volume IV–Mathematical Aspects*. Prentice-Hall, New Jersey, 1983.

[42] J. T. Oden and J. N. Reddy. *An Introduction to the Mathematical Theory of Finite Elements*. John Wiley and Sons, New York, 1976.

[43] Sam Qian and J. Weiss. Wavelet and the numerical solution of partial differential equations. *Journal of Computational Physics*, 106:155–175, 1993.

[44] D. Shepard. A two-dimensional function for irregularly spaced data. In *ACM National Conference*, pages 517–524, 1968.

[45] J. W. Swegle, S. W. Attaway, M. W. Heinstein, F. J. Mello, and D. L. Hicks. An analysis of the smoothed particle hydrodynamics. Technical Report SAND93-2513 UC-705, Sandia, 1994.

[46] M. Tabbara, T. Blaker, and T. Belytschko. Finite element derivative recovery by moving least square interpolants. *Computer Methods in Applied Mechanics and Engineering*, 117:211–223, 1994.

[47] W. Tworzydlo. Analysis of large deformations of membrane shells by the generalized finite difference method. *Computers and Structures*, 27(1):39–59, 1987.

[48] W. Tworzydlo. The fdm in arbitrary curvilinear co-ordinates - formulation, numerical approach and applications. *International Journal for Numerical Methods in Engineering*, 28:261–277, 1989.

[49] J. R. Williams and Amarantuga. Introduction to wavelets in engineering. *International Journal for Numerical Methods in Engineering*, 37:2365–2388, 1994.

[50] Genki Yagawa. Some remarks on free mesh method: A kind of meshless finite element method. In *International Conference on Computational Engineering Science*, Hawaii, USA, August 1995.